Published in final edited form as:
Chem Res Toxicol. 2010 December 20; 23(12): 1890–1904. doi:10.1021/tx1002194.

Inactivation of lipid glyceryl ester metabolism in human THP1 monocytes/macrophages by activated organophosphorus insecticides: Role of carboxylesterase 1 and 2

Shuqi Xie[§], **Abdolsamad Borazjani**[§], **M. Jason Hatfield**[‡], **Carol C. Edwards**[‡], **Philip M. Potter**[‡], and **Matthew K. Ross**[§,*]

[§]Center for Environmental Health Sciences, Department of Basic Sciences, College of Veterinary Medicine, Mississippi State University, P.O. Box 6100, Mississippi State, MS 39762

[‡]Department of Chemical Biology and Therapeutics, St. Jude Children's Research Hospital, 262 Danny Thomas Place, Memphis, TN 38105

Abstract

Carboxylesterases (CES) have important roles in pesticide and drug metabolism, and contribute to the clearance of ester-containing xenobiotics in mammals. Tissues with the highest levels of CES expression are the liver and small intestine. In addition to xenobiotics, CES also harness their broad substrate specificity to hydrolyze endobiotics, such as cholesteryl esters and triacylglycerols. Here we determined if two human CES isoforms, CES1 and CES2, hydrolyze the endocannabinoids 2-arachidonoylglycerol (2AG) and anandamide (AEA), and two prostaglandin glyceryl esters (PG-Gs), which are formed by COX-mediated oxygenation of 2AG. We show that recombinant CES1 and CES2 efficiently hydrolyze 2AG to arachidonic acid (AA), but not amide-containing AEA. Steady-state kinetic parameters for CES1- and CES2-mediated 2AG hydrolysis were, respectively: k_{cat}, 59 and 43min^{-1}; K_m, 49 and 46μM; k_{cat}/K_m, 1.2 and 0.93μM^{-1} min^{-1}. k_{cat}/K_m values are comparable to published values for rat monoacylglycerol lipase (MAGL)-catalyzed 2AG hydrolysis. Furthermore, we show that CES1 and CES2 also efficiently hydrolyze PGE_2-G and $PGF_{2\alpha}$-G. In addition, when cultured human THP1 macrophages were treated with exogenous 2AG or PG-G (10μM, 1h), significant quantities of AA or PGs were detected in the culture medium; however, the ability of macrophages to metabolize these compounds was inhibited (60-80%) following treatment with paraoxon, the toxic metabolite of the insecticide parathion. Incubation of THP1 cell lysates with small-molecule inhibitors targeting CES1 (thieno[3,2-e][1]benzothiophene-4,5-dione or JZL184) significantly reduced lipid glyceryl ester hydrolase activities (40-50% for 2AG and 80-95% for PG-Gs). Immunodepletion of CES1 also markedly reduced 2AG and PG-G hydrolase activities. These results suggested that CES1 is in part responsible for the hydrolysis of 2AG and PG-Gs in THP1 cells, although it did not rule out a role for other hydrolases, especially with regard to 2AG metabolism since a substantial portion of its hydrolysis was not inactivated by the inhibitors. An enzyme (M_r 31-32kDa) of unknown function was detected by serine hydrolase activity profiling of THP1 cells and may be a candidate.

[*]Corresponding author: Matthew Ross, P.O. Box 6100, Mississippi State, MS 39762, Phone Number: 662-325-5482, Fax number: 662-325-1031, mross@cvm.msstate.edu.

Supporting Information
Supplementary Figures 1-7 are available.

Finally, the amounts of *in situ* generated 2AG and PG-Gs in macrophages were enhanced by treating the cells with bioactive metabolites of OP insecticides. Collectively, the results suggest that in addition to MAGL and fatty-acid amide hydrolase (FAAH), which have both been documented to terminate endocannabinoid signaling, CES may also have a role. Furthermore, since PG-Gs have been shown to possess biological activities in their own right, CES may represent an important enzyme class that regulates their in vivo levels.

Keywords

carboxylesterases; endocannabinoids; 2-arachidonoylglycerol; prostaglandin glyceryl esters; THP1 macrophages; organophosphorus insecticides

Introduction

Endocannabinoids are bioactive arachidonoyl derivatives produced on demand in cells that act locally to affect multiple physiological and pathophysiological processes in central and peripheral tissues (1). The two best studied endocannabinoids are 2-arachidonoylglycerol (2AG) and arachidonoyl ethanolamide (AEA). Both lipid mediators bind and activate G-protein coupled receptors known as cannabinoid receptors (CB1 and CB2). CB1 is abundantly expressed in the central nervous system and to a lesser degree in peripheral tissues (2). CB2 receptors, however, are predominantly expressed in macrophages and other immune cells and to a lesser amount in the CNS (3).

Endocannabinoids are also substrates for COXs (4,5) and cytochrome P450s (6), producing glyceryl ester and amide derivatives of prostaglandins (PG-Gs/PG-EAs) and hydroxyeicosatrienoic acid and epoxyeicosatrienoic acid (HETE-Gs/EET-Gs), respectively. Recombinant COX-2 protein was shown to oxygenate 2AG with the same catalytic efficiency as arachidonic acid (AA), whereas COX-1 was less efficient at metabolizing 2AG compared to AA (5). Furthermore, activation of murine RAW 264.7 cells and primary murine peritoneal macrophages with LPS/IFN-γ, followed by treatment with exogenous 2AG or zymosan led to the robust production of PGE_2-G and PGD_2-G, demonstrating that 2AG can be oxygenated to PG-Gs within intact cells (7). It has been speculated that oxygenated PG-G metabolites are produced to regulate the levels of bioactive lipids, such as 2AG, and/or to produce novel endocannabinoid-derived lipid mediators that possess unique receptors and physiological functions (8). In line with this, treatment of RAW macrophages with PGE_2-G was found to increase intracellular Ca^{2+} concentration in a concentration-dependent manner, and Ca^{2+} mobilization was not blocked by PG receptor antagonists suggesting that PGE_2-G did not bind to PG receptors (9). Furthermore, PGE_2-G was shown to be produced endogenously in rat paw and to have roles in pain and inflammation (10). Taken together, these findings indicate that PG-Gs are biosynthesized in vitro and in vivo, bind to unique non-PG receptors, and have biological relevance in health and disease.

Recent findings in animal models of disease suggest that CB1 receptor antagonism can reduce atherosclerosis (11), whereas activation of CB2 receptors by a cannabinoid agonist (Δ^9-THC) is atheroprotective (12). These findings suggest that the endocannabinoid system (ECS) has an important role in vascular homeostasis and that its perturbation may lead to

disease. The ECS is composed of several components, including CB receptors, receptor ligands (2AG and AEA), 2AG and AEA biosynthetic enzymes, transporters for endocannabinoid uptake, and hydrolytic enzymes that degrade 2AG and AEA thereby terminating their actions. Monoacylglycerol lipase (MAGL) and fatty-acid amide hydrolase (FAAH) catalyze the hydrolysis of 2AG and AEA, respectively (13). Although pharmacological agonists and antagonists that target CB receptors have been developed for clinical use, their utility has been limited because of side effects that include cognitive/motility impairment and suicidal ideation, respectively, thus preventing their widespread use. However, an attractive alternative to targeting CB receptors directly is to inhibit the catabolic enzymes MAGL and/or FAAH with pharmacological agents with the intent of increasing endocannabinoid levels in tissues (13).

In addition to MAGL and FAAH, carboxylesterases (CES) are also members of the serine hydrolase superfamily. Satoh and Hosokawa (14) classified mammalian CES into five groups (CES 1-5), based on their amino acid homology. The majority of identified CES fall within the CES1 and CES2 sub-families. CES have a very broad substrate specificity, which is attributed to a large conformable active site that permits entry of numerous structurally diverse substrates, including endobiotics and xenobiotics (15,16). Organophosphate (OPs), carbamate, and pyrethroid insecticides can be metabolized by CES (17-19); however, CES are irreversibly inhibited by OPs during attempted catalytic turnover of these substrates, or reversibly inhibited by carbamates due to slow decarbamoylation rates. There are five CES genes reported in the Human Genome Organization database, although *CES1* and *CES2* are the two best characterized genes (20). CES are widely distributed in several tissues, including liver and intestine, and the hepatointestinal axis is of particular importance in xenobiotic metabolism because of the high concentrations of ester-containing toxins that are ingested orally (21). Although CES1 is found in much greater amounts (~50-fold) than CES2 in human liver (22), CES2 is much more abundant than CES1 in human intestine (23). The high level of CES1 expression in liver was recently underscored by findings of the Human Liver Proteome project, which determined that CES1 was the tenth most abundant protein (out of >6,000) expressed in the human liver (24). Furthermore, CES1 protein is also expressed in human primary monocytes/macrophages and THP1 macrophages, where it functions in part to liberate free cholesterol from neutral lipid droplets (25).

In this study, it was determined whether carboxylesterases are another enzyme family that can catalyze the hydrolysis of endocannabinoids. The specific goals of this study were to establish if 2AG, AEA, and PG-Gs are natural substrates for human carboxylesterases 1 and 2 using both recombinant enzymes and cultured human immune cells (THP1 monocytes/macrophages), and whether the levels of these lipid mediators could be modulated by CES1 inhibition following exposure of THP1 macrophages to bioactive metabolites of OP insecticides. Paraoxon (PO) and chlorpyrifos oxon (CPO) are metabolites of the phosphothionate insecticides parathion and chlorpyrifos, respectively, which are compounds still widely used for pest control resulting in widespread human exposure (26). Bioactive oxon metabolites are formed by P450-mediated biotransformation of phosphothionates in the liver and are potent and non-specific covalent inhibitors of serine hydrolases (27). Covalent modification of serine hydrolases in their native cellular environment may result in

the accumulation of endogenous substrates for these enzymes (e.g., 2AG), thereby modulating physiological homeostasis.

Experimental procedures

Chemicals, cells, and reagents

2AG, AA, AA-d_8, PGE_2-G, $PGF_{2\alpha}$-G, PGE_2, $PGF_{2\alpha}$, and 8-*iso*-$PGF_{2\alpha}$-d_4 were from Cayman Chemicals (Ann Arbor, MI). PO and CPO were kind gifts of Dr. Howard Chambers (Mississippi State University). Trypan Blue solution (0.4% w/v), PMA, β-mercaptoethanol, benzil, phorbol 12-myristate 13-acetate (PMA), fatty-acid free bovine serum albumin (BSA), lipopolysaccharide (LPS), ionomycin, penicillin, streptomycin, indomethacin, and all buffer components were purchased from Sigma (St. Louis, MO). Thieno[3,2-e][1]benzothiophene-4,5-dione (S-3030) was synthesized as previously described (28). JZL184 and WWL70 were purchased from Cayman. The activity-based serine hydrolase probe, fluorophosphonate-biotin (FP-biotin), was from Toronto Research Chemicals (North York, Ontario). HPLC grade solvents were from Burdick and Jackson. Human THP1 monocytes, murine J774 macrophages, RPMI-1640 medium, Dulbecco's Modified Eagle's Medium (DMEM), gentamicin sulfate solution (50 mg/ml), and Hanks' balanced salt solution without calcium, magnesium or phenol red were purchased from the American Type Culture Collection (ATCC) (Manassas, VA). Fetal bovine serum (FBS) was purchased from Invitrogen (Carlsbad, CA). Recombinant human CES1 and CES2 proteins were expressed in baculovirus-infected *Spodoptera frugiperda* cells and purified (29,30). Recombinant human MAGL and FAAH proteins and N-arachidonoyl maleimide (NAM) were from Cayman. Anti-MAGL and anti-FAAH antibodies were from Cayman, anti-CES1 was a kind gift of Dr. M. Hosokawa (Chiba University, Japan), anti-β-actin and anti-COX-2 antibodies were from Santa Cruz Biotechnology.

Culture conditions

THP1 monocytes were grown in suspension in RPMI-1640 medium supplemented with 10% FBS, 0.05 mM β-mercaptoethanol, and 50 μg gentamicin/mL (growth medium) at 37°C and 5% CO_2. The cells were grown at a density between 0.2×10^6 and 1×10^6 cells/ml as recommended by ATCC. THP1 monocytes were differentiated into macrophages by incubating in growth medium containing 100 nM PMA for 48-72 h at 37°C and 5% CO_2. Culture medium was replaced every two days with fresh PMA and growth medium.

Preparation of cell lysates

THP1 monocytes were collected by centrifugation (200 × g for 7 min) and washed with phosphate-buffered saline (PBS). The cells were re-suspended in ice-cold 50 mM Tris-HCl (pH 7.4) buffer and lysed by sonication (four 15 second bursts while on ice). Protein concentrations of cell lysates were determined using the BCA reagent according to the manufacturer's instructions (Pierce, Rockford, IL).

Hydrolysis of 2AG and PG-Gs by recombinant CES1 and CES2 protein

Reactions using recombinant proteins were performed in 50 mM Tris HCl (pH 7.4) buffer with 0.01% fatty-acid free bovine serum albumin (BSA) containing substrate concentrations

varying from 0–250 μM (for PG-Gs) and 0–400 μM (for 2AG) in a total reaction volume of 50 μl. After pre-incubation of buffer and substrate for 5 min at 37°C, reactions were initiated by the addition of recombinant CES1 or CES2 enzyme (0.2 μg) or buffer (non-enzymatic). Reactions were quenched after 10 min with an equal volume of acetonitrile containing 8-*iso*-$PGF_{2\alpha}$ -d_4 (140 pmol, for PG-Gs) or AA-d_8 (500 pmol, for 2AG). Quenched reactions were placed on ice for 15 min, then centrifuged at 16,000 × *g* (4°C, 5 min) prior to transferring supernatants into HPLC vials. Supernatants were analyzed for the hydrolysis products PGE_2, $PGF_{2\alpha}$, or AA by LC-MS (see below for details). Kinetic parameters were determined by performing non-linear regression analysis using the Michaelis-Menten equation with Sigma Plot v. 8.02. The kinetic parameters k_{cat}, K_m, and k_{cat}/K_m were obtained.

2AG hydrolysis by recombinant human CES1 and MAGL following incubation with OP oxons

To compare the inhibition potencies of OP oxons (CPO and PO) toward CES1 and MAGL, reactions were performed in 50 mM Tris-HCl (pH 7.4) buffer containing OP oxon concentrations varying from 0–100,000 nM in a total volume of 50 μl. Recombinant CES1 or MAGL enzymes (0.5 μg) were added to each reaction along with the desired concentration of oxon. After pre-incubation of enzyme and oxon for 15 min at 37°C, reactions were initiated by the addition of 10 μM 2AG. After 15 min, reactions were quenched with an equal volume of acetonitrile containing arachidonic acid–d_8 (AA-d_8, 500 pmol), placed on ice, and centrifuged at 16,000 × *g* (4°C, 5 min). Supernatants were analyzed for AA by LC-MS.

Treatment of THP1 monocyte lysates with oxons, JZL184 or reversible inhibitor S-3030

Control (untreated) THP1 cell lysates were diluted in 50 mM Tris-HCl (pH 7.4) buffer to a final concentration between 0.25-0.50 mg protein/ml. Oxon (PO or CPO), JZL184 or reversible in-hibitor (S-3030) was added from ethanolic or acetonitrile stock solutions to dilute cell lysates to give concentrations indicated in figures. The final concentration of the organic solvent in all reactions was 0.1% (v/v). After pre-incubation times between 5-30 min at 37°C, lipid substrate was subsequently added to yield the indicated final concentrations (2AG, 10 or 25 μM; PGE_2-G and $PGF_{2\alpha}$-G, 10 or 25 μM). After 30-45 min, reactions were terminated by addition of an equal volume of acetonitrile containing deuterated internal standard (8-*iso*-$PGF_{2\alpha}$-d_4 or AA-d_8, 140 pmol).

Detection of serine hydrolases in THP-1 cell lysates using activity-based protein probe FP-biotin

THP1 monocytes lysates (1 mg/ml protein, 25 μl reaction volume, 50 mM Tris-HCl, pH 7.4) were treated with FP-biotin (2 μM final; 1 μl of a 50 μM stock dissolved in DMSO) for 1 h (room temp). Reactions were quenched by adding 10 μL of 6× SDS-PAGE loading buffer (reducing) and heating for 5 min (95°C). Biotinylated proteins were resolved by SDS-PAGE and detected with avidin-HRP as described in detail in (31). In certain reactions, THP1 lysates were preincubated for 30 min with the irreversible inhibitors PO, CPO or JZL184, followed by addition of FP-biotin (2μM) and incubation for 1h (room temp). For the

reversible inhibitor S-3030, lysates were treated sequentially with S-3030 and FP-biotin (0.2 μM) and incubation for 7.5 min, a time pre-judged to permit visualization of the biotinylated CES1 product by avidin-HRP blotting although the reaction between enzyme and FP-biotin had not proceeded to completion.

PG-G and 2AG hydrolysis by immunodepleted THP1 monocyte lysates

THP1 monocyte lysates, solubilized in 50 mM Tris-HCl (pH 7.4) containing 0.5% w/v Brij (mixed gently for 1h, 4°C), were incubated overnight with preimmune IgG (used as control) or anti-CES1 IgG in the presence of protein A-agarose beads to deplete CES1, as described in detail in (31). PG-Gs or 2AG were then added to the immunodepleted THP1 cell lysate to determine the extent of their hydrolysis. Briefly, triplicate reactions were performed in 50 mM Tris-HCl (pH 7.4) buffer containing 25 μM PG-Gs or 10 μM 2AG in a total reaction volume of 50–125 μl. After pre-incubation of buffer and substrate for 5 min at 37° C, reactions were initiated by the addition of 10-30 μg of control or immunodepleted THP1 cell lysate. Reactions were quenched after a 30 min incubation with an equal volume of acetonitrile containing internal standard 8-*iso*-$PGF_{2\alpha}$-d_4 (140 pmol) and placed on ice for 10 min. Samples were centrifuged at 16,000 × *g* (4°C, 5 min) to remove precipitated protein prior to transferring supernatants into HPLC vials. Supernatants were analyzed by LC-MS to quantify the hydrolysis products PGE_2, $PGF_{2\alpha}$, or AA.

Western blot analysis of CES1, FAAH, and MAGL

THP1 macrophage lysate proteins were separated by SDS-PAGE. Following electrophoretic transfer, PVDF membranes were probed with rabbit anti-CES1 (1:4000 v/v), rabbit anti-FAAH (1:250 v/v), or rabbit anti-MAGL (1:133 v/v) for 1 h at room temperature. Membranes were washed, followed by incubation with goat anti-rabbit secondary antibody conjugated to HRP (1:20,000 v/v). The chemiluminescent signal was recorded using X-OMAT photographic film (Eastman Kodak Co., Rochester, NY). Increasing amounts of recombinant CES1 and MAGL (1-50 ng) were used on gels as calibrants for quantitative immunoblots. In certain cases, rabbit anti-βactin was included to verify equal protein loading on gels.

Sequential treatment of intact THP1 cells with oxon followed by 2AG and PG-Gs

Monocytes—THP1 monocytes (2×10^6 cells in 2-ml serum-free culture medium) were placed into wells of a 6-well plate. Paraoxon was added to wells to give a final concentration of 1 μM, whereas controls received solvent vehicle (ethanol); the final concentration of ethanol in each well was 0.1% (v/v). Cells were exposed to paraoxon for 30 min and subsequently treated for 60 min with 2AG, PGE_2-G, or $PGF_{2\alpha}$-G (25 μM each). Following treatments, cells were pelleted and the culture medium removed for analysis. The cells were washed three times with ice-cold PBS, re-suspended in 50 mM Tris-HCl (pH 7.4) buffer, and lysates prepared by sonication as described above. Carboxylesterase activity of the lysates was determined using *p*-nitrophenyl valerate as substrate to verify inhibition by oxon (31). The culture medium was spiked with internal standard (AA-d_8, 500 pmol) and extracted with 3 volumes of ethyl acetate containing 0.1% acetic acid. The ethyl acetate layer was recovered and evaporated to dryness under nitrogen. The residues were

redissolved in 100 μl of acetonitrile:water (1:1, v/v), filtered through a microfuge filter unit (0.22 μm), and transferred to LC vials for LC-MS analysis.

Macrophages—THP1 monocytes (~3×10^6 cells) were plated into 6-well dishes in complete growth medium and differentiated into macrophages by addition of PMA (70 nM) for 48-72 h. After the cells had differentiated, the culture medium was removed and cells washed with Hank's buffer. Cells were then overlaid with serum-free culture medium containing PO (0.1-10 μM) or vehicle (ethanol) and incubated for 30 min. 2AG was then directly added to the culture medium (10 μM) and incubation continued for another 60 min. Cells and medium were then combined with AA-d_8 (500 pmol) and extracted with ethyl acetate (0.1% acetic acid) as described above for LC-MS analysis.

In situ formation of PG-Gs by THP1 macrophages

THP1 monocytes (~$3\text{-}5\times10^6$ cells) were plated into 60-mm dishes in complete growth medium and differentiated into macrophages by the addition of PMA (70 nM) for 48-72 h. After the differentiation period, culture medium was removed and cells washed with Hank's buffer. Fresh serum-free culture medium supplemented with lipopolysaccharide (LPS, 1 μg/ml) was added to the cells. After 5 h incubation with LPS, the culture medium was discarded and the cells were washed with Hank's buffer or PBS. The macrophages were then pre-treated with oxons (CPO or PO, 1 μM) or vehicle (ethanol, 0.1% v/v) in fresh serum-free medium for 30 min. After 30 min, 2AG (10 μM) or ionomycin (5 μM) was added to the culture medium and the cells incubated for an additional 30 min. Ionomycin stimulates macrophages to biosynthesize 2AG from endogenous arachidonic acid-containing phospholipids (53). In some experiments, a non-specific COX inhibitor, indomethacin, was added to the culture medium at the same time as the oxons to give a final concentration of 3 μM. After incubation with 2AG or ionomycin, the culture medium was removed and spiked with internal standards (8-iso-$PGF_{2\alpha}$-d_4 and 2AG-d_8; 7 pmol and 50 pmol, respectively). The medium was extracted with 3 volumes of ethyl acetate (containing 0.1% acetic acid) and the ethyl acetate fraction was evaporated to dryness under nitrogen. The residues were resuspended in 100 μl of 1:1 methanol: water and the extract analyzed by LC-MS/MS.

LC-MS analytical procedures

Analysis of products obtained from recombinant enzyme-catalyzed reactions and THP1 cell/medium extracts was performed on a Thermo MSQ single-quadrupole system interfaced with a Surveyor LC pump (Thermo Fisher Scientific, San Jose, CA). The mobile phases were a blend of solvent A (0.1% v/v acetic acid in water) and solvent B (0.1% v/v acetic acid in acetonitrile). Samples (20 μL) were injected onto a C18 column (2.1 mm × 100 mm, Thermo) equipped with guard column and analytes were eluted with the following gradient program: 0 min (95% A, 5% B), 0.5 min (95% A, 5% B), 10 min (0% A, 100% B), 15min (0% A, 100% B), 20 min (95% A, 5% B). Flow rate was 0.5 mL/min and the column eluate was directed into the mass spectrometer. Ions were introduced into MS by electrospray ionization in positive or negative ion modes. The MS single quadrupole was operated in single-ion mode (SIM) to detect the following ions: AA ($[M\text{-}H]^-$ *m/z* 303), 2AG ($[M+H]^+$ *m/z* 379.3), $PGF_{2\alpha}$ ($[M\text{-}H]^-$ *m/z* 353.2), and PGE_2 ($[M\text{-}H]^-$ *m/z* 351.2). Internal standards

included AA-d_8 (*m/z* 310) and 8-iso-$PGF_{2\alpha}$-d_4 (*m/z* 357), which were used to quantify the amounts of AA and PGs.

Extracts of culture medium from LPS-pretreated macrophages that had been stimulated to produce PG-Gs were analyzed by UPLC-MS/MS. In brief, a Waters Acquity UPLC was interfaced with a Thermo Quantum Access triple-quadrupole mass spectrometer. The mobile phase was a blend of solvent A (2 mM ammonium acetate/0.1% acetic acid in water) and solvent B (0.1% acetic acid in methanol). Samples (10 μL) were injected into an Acquity UPLC BEH C18 column (2.1 × 50 mm, 1.7 μm) equipped with VanGuard pre-column (2.1 × 5 mm, 1.7 μm), and analytes were eluted with the following gradient program: 0 min (95% A, 5% B), 0.5 min (95% A, 5% B), 5 min (5% A, 95% B), 6 min (5% A, 95% B), 7 min (95% A, 5% B), 8 min (95% A, 5% B). Flow rate was 0.4 mL/min and the entire column eluate was directed into the mass spectrometer (heated electrospray ionization in positive ion mode). Single reaction monitoring (SRM) of ammoniated adducts of each analyte were as follows: $PGF_{2\alpha}$-G, $[M+NH_4]^+$ *m/z* 446.4>393.3; PGE_2-G, $[M+NH_4]^+$ *m/z* 444.4>391.3; 2AG, $[M+NH_4]^+$ *m/z* 396.3>287.3; and 2AG-d_8, $[M+NH_4]^+$ *m/z* 404.3>295.3 (32). Scan times were 0.2 s per SRM and scan width was 0.01 m/z. Collision energies and tube lens voltage were optimized using autotune software for each analyte by post-column infusion of individual compounds into 50% A/50% B mobile phase, pumping at a flow rate 0.4 ml/min. The source settings were as follows: spray voltage, +4000V; vaporizer temp, 350°C; capillary temp, 285°C; sheath gas pressure, 50 psi; aux gas pressure, 5 psi.

Calibration standards containing each analyte were routinely prepared in serum-free RPMI culture medium at 4 different concentration levels (1, 0.1, 0.01, and 0.001 μM). Fortified culture medium was spiked with internal standards (8-iso-$PGF_{2\alpha}$-d_4 and 2AG-d_8, 7 pmol and 50 pmol, respectively) and extracted with ethyl acetate, as described above.

Results

Hydrolysis of 2AG and PG-Gs by recombinant human CES1 and CES2: comparison to MAGL and FAAH

Recombinant CES1 and CES2 enzymes can hydrolyze the ester-containing 2AG to AA and glycerol (see Fig. 1A,B; mass chromatograms for AA obtained from CES1-catalyzed hydrolysis of 2AG are shown in Fig. 1B). However, neither enzyme could hydrolyze the amide-containing AEA. The extent of 2AG hydrolysis by each recombinant CES was protein concentration-dependent (data not shown), time-dependent (CES1 data shown in Fig. 1C), and 2AG concentration-dependent (Fig. 1D). Steady-state Michaelis-Menten kinetic parameters for CES1 and CES2 are reported in Table 1. The turnover number (k_{cat}) for CES1 is greater than CES2, but there was not a marked difference between the catalytic efficiencies (k_{cat}/K_m) for CES1 and CES2. Furthermore, k_{cat}/K_m values for human CES1- and CES2-catalyzed hydrolysis of 2AG were comparable to rat MAGL (2.1 $min^{-1}\mu M^{-1}$; 33) and human MAGL (0.73±0.43 $min^{-1}\mu M^{-1}$; this study), suggesting that human CES enzymes might contribute to 2AG metabolism in vivo.

Prostaglandin glyceryl esters, PGE_2-G and $PGF_{2\alpha}$-G, are formed by COX-mediated oxygenation of 2AG and retain the esterified glycerol moiety (5). We next showed that

recombinant CES1 and CES2 enzymes could hydrolyze PGE_2-G and $PGF_{2\alpha}$-G to their respective free prostaglandins. Analysis of substrate concentration-velocity plots yielded Michaelis-Menten parameters for CES1- and CES2-mediated PG-G hydrolysis that are reported in Table 1. As judged by k_{cat}/K_m values, hydrolysis rates for PGE_2-G and $PGF_{2\alpha}$-G were not significantly different when using CES1 as catalyst, but $PGF_{2\alpha}$-G was hydrolyzed significantly faster (6.5-fold) than PGE_2-G when using CES2. Also, $PGF_{2\alpha}$-G was hydrolyzed three times faster by CES2 than CES1 (Table 1).

Recombinant rat MAGL and FAAH enzymes were previously reported to hydrolyze 2AG and PG-Gs (PGE_2-G and $PGF_{2\alpha}$-G) (33), but this is the first time that these lipid mediators have been reported to be substrates for human CES1 and CES2. Therefore, we compared recombinant forms of human MAGL, FAAH, and CES1 for their ability to hydrolyze a fixed amount of each substrate (Fig. 1E-G). The three enzymes appeared to hydrolyze 2AG at comparable rates when normalized per nmol of enzyme (Fig. 1E), with CES1 exhibiting slightly higher activity than FAAH and MAGL. For the PG-Gs, the rank order of hydrolysis rates was as follows: MAGL>CES1>>FAAH (Fig. 1F,G). MAGL was 2- and 4-fold more active than CES1 when hydrolysis rates of PGE_2-G and $PGF_{2\alpha}$-G were compared, respectively. In contrast to MAGL and CES1, FAAH had little activity toward either PG-G substrate. Also, it was found that human MAGL could metabolize PG-Gs 13-25–fold more rapidly than rat MAGL when k_{cat}/K_m values for rat MAGL and human MAGL were compared (33; current study): $PGF_{2\alpha}$-G, 0.027 and 0.36 $min^{-1}\mu M^{-1}$ for rat and human MAGL, respectively; PGE_2-G, 0.064 and 1.6 $min^{-1}\mu M^{-1}$ for rat and human MAGL, respectively. On the other hand, rat MAGL hydrolyzed 2AG 2.9-fold more efficiently than human MAGL (compare 2.1 and 0.73 $min^{-1}\mu M^{-1}$ for rat and human MAGL, respectively).

Cultured human THP1 monocytes hydrolyze exogenous 2AG and PG-Gs

Intact THP1 monocytes could hydrolyze synthetic 2AG or PG-Gs when each of these compounds was added to serum-free culture medium (25 μM final concentration). Significant quantities of 2AG-derived AA or PG-G-derived PGs were detected in the culture medium at the end of 1 h incubations (see Fig. 2A for mass chromatograms of AA obtained from vehicle- and 2AG-treated THP1 monocytes). Note the large amount of AA detected in the 2AG-treated sample but the lack of AA in the vehicle-treated sample. To ensure that measured AA and PGs were obtained by metabolism of 2AG and PG-Gs by THP1 cells, 2AG or PG-G were added to serum-free culture medium in the absence of THP1 cells; negligible amounts of AA or PGs were formed during the incubation period (data not shown). These results clearly demonstrated that intact THP1 monocytes could hydrolyze exogenous 2AG and PG-Gs. Furthermore, similar findings were obtained when using THP1 macrophages instead of monocytes (see below).

Inhibition of CES1 activity by small-molecule inhibitors (S-3030 and JZL184)

CES1, but not CES2, is robustly expressed in cultured human THP1 monocytes/macrophages (31). When cell lysates of untreated THP1 monocytes were incubated with a CES1 inhibitor, S-3030 (28), in the presence of 2AG, PGE_2-G, or $PGF_{2\alpha}$-G, substantial reductions in 2AG and PG-G hydrolysis rates were noted (maximal inhibition using 100 μM S-3030: 55%, 80%, and 97% for 2AG, $PGF_{2\alpha}$-G and PGE_2-G, respectively; Fig. 2B). This

result suggested that CES1 is in part responsible for the hydrolysis of 2AG and PG-Gs in THP1 cells, although it did not rule out a role for MAGL or other hydrolases, especially with regard to 2AG metabolism since a substantial portion of 2AG hydrolytic activity was not inhibited by S-3030.

To further investigate the serine hydrolases present in THP1 cells, monocyte lysates were treated with the activity-based protein probe FP-biotin (51). Following separation of treated proteins by SDS-PAGE, the biotinylated proteins were detected by avidin-HRP blotting. CES1 and a 31-32kDa enzyme were robustly labeled by FP-biotin in their native form (Fig. 2C); however, both enzymes were not labeled when lysate was heated before addition of FP-biotin, demonstrating that the enzymes needed to be active to be labeled. Although a complete list of off-target hydrolases for the CES1 inhibitor S-3030 are not known at this time, it is important to note that S-3030 did not inhibit recombinant human MAGL activity (Supplementary Fig. 2A), thus MAGL does not appear to be an off target for this inhibitor. Moreover, although identifying off-targets for reversible inhibitors such as S-3030 is more challenging than for covalent inhibitors using activity-based protein probes, a competitive kinetic assay was performed using THP1 cell lysate and S-3030 (0-100 μM) and FP-biotin (0.2 μM, 7.5 min reaction time; Supplementary Fig. 2B). The data indicate that native CES1 is inhibited by S-3030 (IC_{50} ~23μM), but the 31-32 kDa enzyme is not, thus it does not appear to be an off target enzyme for S-3030.

The 31-32kDa enzyme observed on the activity gel (Fig. 2C) resembled the migration and doublet behavior of MAGL (47). However, this enzyme does not appear to be MAGL based on the following lines of evidence. First, MAGL has a molecular weight of 35-36kDa (ref. 35 and Supplementary Fig. 4B), not 31-32kDa. Second, after stripping the blot in Fig. 2C, the 31-32kDa enzyme was not immunoreactive toward a human MAGL antibody raised against the N-terminal peptide in MAGL (amino acids 1-14) (data not shown). Third, the 31-32kDa enzyme was not inhibited by the potent MAGL inhibitor JZL184 at concentrations as high as 100 μM, as judged using FP-biotin as an activity probe (Fig. 2D). JZL184 is a carbamate inhibitor that covalently modifies the active-site serine residue in MAGL, thus preventing FP-biotin from reacting with this amino acid (34). Furthermore, the 31-32kDa enzyme is not particularly sensitive to CPO; indeed, high micromolar concentrations (>10 μM) were needed to reduce its activity toward FP-biotin, whereas CES1 was completely inhibited (Supplementary Fig. 1A,C). As shown below and by others (47), MAGL is very sensitive to inhibition by CPO, so there appears to be a differ-ence in the sensitivities of MAGL and the 31-32kDa enzyme toward this oxon. Therefore, based on FP-biotin activity assays and the fact that 2AG hydrolysis activity in THP1 cells cannot be fully ablated by S-3030 or by activated organophosphates at concentrations that inhibit CES1 (Supplementary Fig. 3A,C), these findings are suggestive of a role for the 31-32kDa enzyme in 2AG hydrolysis in THP1 cells. However, in the absence of inhibitors or siRNA that selectively inactivate the 31-32kDa enzyme, one cannot rule out other enzymes at this time.

Interestingly, we also found that JZL184 can potently inhibit both recombinant human CES1 activity using *p*NPV as substrate (data not shown) and native CES1 in THP1 lysates (IC_{50}<0.1μM, Fig. 2D), thus we determined what effect JZL184 had on 2AG and PG-G hydrolysis activity of THP1 monocyte lysates. Inhibition of CES1 in THP1 monocyte

lysates by JZL184 led to maximal reductions of 2AG and PGF2α-G hydrolytic activity of 40% and 80%, respectively (Fig. 2E). Importantly, the activity blot in Fig. 2D showed that JZL184 as low as 0.1 μM can completely inhibit CES1 but not the 31-32kDa enzyme in THP1 cell lysate. Based on results obtained with S-3030 and JZL184, CES1 is in part responsible for the hydrolysis of 2AG (40-50%), and is a major hydrolase (80-95%) of PG-Gs in THP1 cells. Moreover, these results are also consistent with the notion that the 31-32kDa enzyme is a possible candidate responsible for the JZL184-insensitive glyceryl ester hydrolytic activity in THP1 cells.

Expression of MAGL, FAAH, and CES1 in human THP1 monocytes/macrophages

Western blotting of THP1 cell lysate proteins was done to examine the levels of hydrolytic enzymes implicated in endocannabinoid and PG-G catabolism. The results show that CES1 and MAGL proteins were expressed in THP1 macrophages, whereas FAAH was not detectable (Fig. 3A). Similar expression patterns were also noted in THP1 monocytes. Moreover, the absolute amount of CES1 in THP1 macrophages was 1.12±0.05 μg/mg lysate protein (18.7±0.8 pmol/mg lysate protein), whereas the level of MAGL was 28.4±7.6 ng/mg lysate protein (0.81±0.22 pmol/mg lysate protein) when quantitative immunoblotting was performed (mean±SD, *n*=3; Supplementary Fig. 4A,B). Thus, CES1 is expressed at levels 23-fold greater than MAGL in THP1 macrophages when molar amounts of enzyme are compared, whereas FAAH is undetectable.

Blankman et al. showed that ABHD6 (38kDa) is a minor player in the hydrolytic metabolism of 2AG in mouse brain (48). To determine whether ABHD6 is present in THP1 cells, we transfected COS7 cells with human ABHD6 cDNA and examined its expression using FP-biotin. Based on its migration behavior in SDS-PAGE, ABHD6 does not appear to be expressed in THP1 monocytes/macrophages (Supplementary Fig. 5A). Moreover, we also treated THP1 cell lysates with a specific ABHD6 inhibitor (WWL70; 48) and found that this compound did not inhibit 2AG hydrolytic activity (Supplementary Fig. 5B). Both lines of evidence are consistent with ABHD6 not being expressed in the THP1 cell line. In addition, ABHD12 (45kDa) is another enzyme implicated in 2AG hydrolysis. However, inspection of Figure 3 from Blankman et al. (48) and comparison with our own activity blots (Figure 2C) indicates that ABHD12 is also not expressed in THP1 cells. Thus, it is unlikely that ABHD6 and ABHD12 contribute to 2AG hydrolysis in THP1 cells.

Hydrolysis of 2AG and PG-Gs by recombinant enzymes, THP1 monocyte lysates, and intact cells: inhibition of this activity by bioactive metabolites of OP insecticides

Inhibition of recombinant CES1 and MAGL—The extent of inhibition of human CES1 and MAGL activity by two bioactive insecticide metabolites, PO and CPO, was determined. Each enzyme was pretreated with increasing amounts of PO and CPO for 15 min, followed by addition of 2AG substrate (10 μM). The results showed that CES1 is much more sensitive to inhibition by PO when compared to MAGL, whereas CPO can inhibit both enzymes although CES1 appeared to be more sensitive than MAGL based on IC_{50}s (Fig. 3B,C). Even at high concentrations of PO, very little inhibition of human MAGL is seen (IC_{50} >10,000 nM; Fig. 3C). It was also found in our study that a widely used small-molecule inhibitor of MAGL, N-arachidonoyl maleimide (NAM), inhibited recombinant

CES1 activity toward 2AG (Supplementary Fig. 2A). Moreover, as already mentioned above, JZL184 (34) also inactivates human CES1 activity, which is consistent with a previous report that showed murine CES1 orthologs were inhibited by this compound (35). Therefore, since CES1 appears to be an off target for these two MAGL inhibitors, and the fact that PO can potently inhibit CES1 but not MAGL, the activities of MAGL and CES1 in THP1 cells may be distinguished by using PO as a "selective" CES1 inhibitor.

Hydrolysis of 2AG and PG-Gs by THP1 monocyte lysate after pretreatment with PO or CPO—We hypothesized that since MAGL and CES1 are both inhibited by CPO, whereas only CES1 is inhibited by PO, differential inhibition of 2AG hydrolysis activity would be observed when THP1 cell lysate proteins were treated with these oxons at a concentration of 1 μM. It should be noted here that the 31-32kDa enzyme is not inhibited by either oxon at this concentration, based on FP-biotin activity gels (Supplementary Fig. 1A,B). Following pretreatment of lysates with PO or CPO (1 μM), hydrolysis of exogenous 2AG (10 μM) was significantly inhibited compared to control (35% and 49% for PO and CPO, respectively; $p<0.05$; Supplementary Fig. 3A). Similar results were found when intact THP1 monocytes were pretreated with 1 μM PO or CPO before adding 2AG to the cells (Supplementary Fig. 3C). However, essentially no difference in inhibition potency was observed for the two oxons at 1 μM using either cell lysates or intact cells, which suggested that MAGL did not play a significant role in 2AG hydrolysis in THP1 cells because 1 μM CPO would have been expected to completely inhibit any MAGL contribution. Increasing CPO to 10 μM in cell lysates caused a further decrease in 2AG hydrolysis activity (72% inhibition, $p<0.05$), whereas increasing PO to 10 μM did not further enhance inhibition (Supplementary Fig. 3A). When THP1 monocyte lysate was titrated with high concentrations of CPO, the 2AG hydrolysis activity was maximally knocked down by 94% at 500 μM. On the other hand, 2AG hydrolysis activity was knocked down by 55% with 500 μM PO. It was also noted that PO and CPO (1 μM) caused near complete inhibition of PGE_2-G hydrolysis activity in THP1 cell lysate (Supplementary Fig. 3B). This was consistent with the result in Fig. 2B, which showed that S-3030 could inhibit >95% of the PGE_2-G hydrolytic activity in THP1 cell lysate.

Hydrolysis of 2AG and PG-Gs by intact THP1 monocytes and macrophages following pretreatment with PO—Following pretreatment of intact THP1 monocytes with PO (1 μM, 30 min) the ability of the cells to hydrolyze exogenous 2AG, PGE_2-G, or $PGF_{2\alpha}$-G (25 μM, 60 min) was found to be significantly inhibited by ~50% ($p<0.05$) (Supplementary Fig. 6). Further, pretreatment of intact THP1 macrophages with increasing amounts of PO prior to addition of synthetic 2AG or PG-Gs caused a concentration-dependent inhibition of 2AG hydrolysis activity (Fig. 4) and PG-G hydrolysis activity (Fig. 5A,B). Significant inhibition in hydrolytic activities was seen at PO concentrations as low as 100 nM ($p<0.05$), which again indicates that CES1 has a role in the metabolism of these lipid mediators. In addition to concentration-dependent reductions in AA levels, concomitant increases in 2AG amounts were also observed (Fig. 4), indicating that exposure of THP1 macrophages to PO causes endocannabinoid stabilization. Similar stabilization was seen with PG-Gs following treatment of cells with PO.

Immunoprecipitation of CES1 from cell lysates

Attempts were made to knockdown CES1 gene expression in THP1 macrophages with shRNA constructs but this proved unsuccessful, which is not surprising considering the difficulties that are encountered when transfecting macrophages. Therefore, we instead immunoprecipitated CES1 protein from THP1 cell lysates. Immunoprecipitation of CES1 from THP1 monocyte lysates was confirmed by western blotting of supernatants, yet β-actin and MAGL were detectable in both the control and CES1 depleted lysates (see Fig. 6A). Furthermore, supernatants were treated with FP-biotin and proteins resolved by SDS-PAGE. As can be seen from the activity gel in Fig. 6B, CES1 was completely depleted when cell lysate was incubated with CES1 specific antibody, but not from lysate incubated with non-specific antibody. In addition, the 31-32kDa enzyme is present in near equal amounts in both supernatants, indicating that is was not precipitated by the CES1 antibody. The hydrolysis activity of the CES1-depleted lysate toward PGE_2-G and $PGF_{2\alpha}$-G was reduced 80% and 50%, respectively (Fig. 6C,D). In addition, the 2AG hydrolysis activity was reduced on average by 64% when 2AG was added to immunodepleted lysates (Fig. 6E). These data are consistent with the notion that CES1 has a role in the catabolism of PG-G and 2AG in the THP1 cell line. It was also noticed that solubilization of THP1 lysate proteins using the non-ionic detergent Brij appeared to reduce the activity of the 31-32 kDa enzyme but not CES1, as judged by the FP-biotin activity experiments (Fig. 6B). This may account for why the relative amount of 2AG hydrolytic activity knocked down by CES1 immunoprecipitation (64%) was greater than the knock down caused by small molecule inhibitors that apparently completely inhibit CES1 (0.5μM JZL184, 40% inhibition; 100μM S-3030, 50% inhibition; 1μM PO, 35% inhibition).

In situ generation of PGF_{2a}-G and PGE_2-G in J774 and THP1 macrophages

To address the physiological relevance of these findings, murine J774 macrophages could be stimulated to produce $PGF_{2\alpha}$-G and PGE_2-G by priming cells with LPS (1 μg/ml) then treating with either 2AG (10 μM) or ionomycin (5 μM) (Fig. 7 A,B; data shown for $PGF_{2\alpha}$-G). This confirmed previous studies that used RAW cells and primary murine macrophages (5,7). Our initial attempts to stim-ulate human THP1 macrophages to produce PG-Gs in the same manner did not yield detectable amounts of these compounds. However, if LPS-pretreated THP1 macrophages were exposed to bioactive metabolites of OP insecticides for 30 min prior to adding exogenous 2AG (10 μM), then $PGF_{2\alpha}$-G and PGE_2-G accumulated in the culture medium (Fig. 7C-F and Fig. 8). If oxon was not added to the culture medium, then PG-Gs were detected at levels close to the detection limit of the LC-MS/MS assay; however, addition of 1 μM PO to macrophages for 30 min prior to addition of 10 μM 2AG caused a 4-fold and 2-fold increase in $PGF_{2\alpha}$-G and PGE_2-G levels, respectively (Fig. 8). Furthermore, addition of the non-selective COX inhibitor indomethacin blocked formation of PG-Gs by THP1 macrophages (Fig. 7E), which is consistent with previous reports that used murine macrophages (7).

It was also found that CPO and PO had differential effects on the amounts of PG-Gs and 2AG formed when LPS-primed THP1 macrophages were stimulated with ionomycin (Fig. 9). First, as expected, it was shown that LPS priming of THP1 macrophages led to robust induction of COX-2 (Fig. 9A). Next, treatment of LPS-primed macrophages with 1 μM CPO

significantly elevated $PGF_{2\alpha}$-G, PGE_2-G, and 2AG levels compared to vehicle-treated cells following ionomycin stimulation (Fig. 9B). In contrast, treatment of cells with 1 μM PO did not significantly elevate the amounts of PG-Gs and 2AG compared to vehicle treated cells (Fig. 9C). These differing results likely occurred because CPO is a more potent inhibitor of glyceryl ester metabolism than PO within intact cells. Taken together, treatment of THP1 macrophages with CPO appeared to prevent the degradation of PG-Gs when produced from either exogenous or endogenous sources of 2AG, whereas PO appeared to block the degradation of PG-Gs only when they were produced from exogenous 2AG (Fig. 8). When PG-Gs were generated in macrophages following ionomycin stimulation, PO did not augment their levels (Fig. 9C).

When THP1 macrophages were cholesterol loaded and subsequently treated with CPO or PO (0, 1 and 10 μM) for 24 h, increasing amounts of 2AG were found to accumulate in the culture medium (Supplementary Fig. 7A,B). For the 1 μM and 10 μM CPO treatment groups, the amounts of 2AG were 2.5-fold and 8.1-fold higher than the control group, respectively. In contrast, 1 μM and 10 μM PO resulted in 3.1-fold and 3.5-fold increases in 2AG levels, respectively. This result suggested that THP1 foam cells are capable of 2AG biosynthesis and secretion without having to be stimulated with agonists such as ionomycin. It further showed that oxon-mediated inhibition of catabolic enzymes in foam cells can contribute to the buildup of the endocannabinoid 2AG in culture medium in a dose-dependent manner. Exposure of THP1 macrophage foam cells to OPs for 24h did not alter CES1 protein levels (Supplementary Fig. 7C)

Discussion

Endogenous cannabinoids are lipid mediators that modulate several physiological functions, including reproduction, motor control, appetite, cognition, analgesia, peripheral metabolism and inflammation (1,36,37). The two most widely studied endocannabinoids, 2AG and AEA, are produced on demand, act locally on CB receptors, and their physiological actions are terminated by hydrolytic enzymes, the best characterized to date being MAGL and FAAH. One of the main findings of this study is that human CES1 and CES2 can effectively hydrolyze 2AG to AA and glycerol. Furthermore, the catalytic efficiencies of recombinant CES1 and CES2 for this activity are similar to or better than recombinant rat MAGL and FAAH (33). Another significant finding is that CES1 and CES2 also efficiently hydrolyze PGF2α-G and PGE2-G, which are COX-mediated oxygenation products of 2AG. Since PG-Gs have been shown to possess biological activities in their own right (9,10,38), CES may represent an important enzyme class that regulates the in vivo levels of these compounds. Therefore, CES might be an attractive target for selective inhibitors with the goal of increasing endocannabinoid and/or PG-G levels in macrophages, thereby modulating lipid glyceryl ester homeostasis. This is the first report to suggest that 2AG and PG-Gs are substrates for human CES1 and CES2, although we previously reported that a bacterial CES (pnbCE) could hydrolyze 2AG (39). Furthermore, it was previously reported that PG-Gs are more rapidly degraded in rat serum than human serum (40). The most likely explanation for this finding is that rat serum contains a CES enzyme that can metabolize PG-Gs, whereas human serum does not (41).

Endocannabinoids have well-described activities in the brain, including a role for 2AG in retrograde signaling between neurons (2). However, they also have physiological roles in the vasculature that may modulate development of atherosclerosis. For example, activation of macrophage CB1 receptors led to increased expression of pro-inflammatory genes (42) and scavenger receptors (43), decreased expression of cholesterol transporters (43), and increased reactive oxygen stress (44). By contrast, CB2 receptor activation had opposing effects on these proatherogenic pathways in macrophages (45,46). Therefore, the local concentration of 2AG in the vessel wall may be an important determinant of foam cell formation and atherosclerosis. To address this issue, we used THP1 macrophages as a model system to examine the metabolism of 2AG and its COX-mediated PG-G metabolites. In our study, intact THP1 macrophages were shown to effectively hydrolyze exogenously added 2AG and PG-Gs, yielding AA and PGs, respectively; however, this ability was significantly reduced in a dose-dependent manner by the organophosphate metabolite PO (Fig. 4,5). Interestingly, human MAGL was found to be insensitive to the inhibitory effects of PO (IC_{50}>10,000 nM), whereas CES1 was inhibited by this compound (IC_{50}=77 nM; Fig. 3). Our initial interpretation of these results was that inhibition of lipid glyceryl ester hydrolysis by PO in intact monocytes (Supplementary Fig. 6) and macrophages (Fig. 4,5) was due to CES1 inactivation, not MAGL. Surprisingly, although serine hydrolase activity profiling of THP1 monocytes/macrophages indicated that CES1 was readily detectable, MAGL activity was not (although it was detected by immunoblotting; Fig. 3A). Furthermore, a 31-32kDa serine hydrolase was clearly evident in Fig.2C, which resembled the migration and doublet behavior of MAGL. However, it could not be inhibited by JZL184 (Fig. 2D) and was relatively insensitive to oxons (Supplementary Fig.1A-D). Based on the use of CES1 chemical inhibitors (S-3030, JZL184, and PO), we conclude that CES1 is responsible for 40-50% and 80-95% of the metabolism of 2AG and PG-Gs in THP1 cells, respectively. As for the remaining hydrolytic activity not attributable to CES1, the 31-32kDa enzyme may be a candidate because it cannot be inhibited by JZL184 and oxons (at low concentrations), but it can be inhibited by high concentrations of oxons (>10μM), which somewhat resembles the inhibition of 2AG metabolism by these compounds. Although the identity of the 31-32kDa enzyme is presently unclear, based on related sequences to MAGL it may be a lysophospholipase-like protein (http://www.uniprot.org/uniprot/Q2VYF8). This putative protein has a predicted molecular weight of 30,720 Da. Interestingly, except for the first 51 amino acids, the remaining primary sequence of Q2VYF8 is identical to human MAGL. The difference in amino terminal sequences between the two proteins might explain the lack of immunoreactivity toward the commercial MAGL antibody, which was raised against an N-terminal peptide of MAGL. This epitope appears to be lacking in the 31-32kDa enzyme. Furthermore, the different N-terminal domain in Q2VYF8 may account for its lack of inhibition by JZL184. Future studies on this protein may be warranted to characterize its function in macrophages.

In contrast to the “selectivity” shown by PO, which inhibited the hydrolytic activity of CES1 but not MAGL, CPO could potently inhibit both recombinant MAGL and CES1 (Fig. 3B,C). Con-sistent with this, it was previously shown that CPO and PO had different inhibition profiles against MAGL, FAAH, and AChE in mouse brain, with CPO considered to be a non-selective agent since it inhibited all three enzymes with low IC_{50}s, and PO considered a

selective inhibitor against AChE compared to MAGL and FAAH (47). Based on western blot data (Fig. 3A) and activity profiling (Fig. 2C), MAGL is expressed in THP1 cells at significantly lower levels than CES1 and FAAH is not detectable. Therefore, it seems that MAGL and FAAH do not contribute significantly to overall lipid glyceryl ester metabolism in this cell line. Nevertheless, PO and CPO were used to study lipid glyceryl ester hydrolysis in intact THP1 macrophages because of potential human exposure to these compounds in the environment. Addition of exogenous 2AG to CPO- and PO-pretreated THP1 macrophages (LPS primed) caused a significant buildup of PG-Gs in the culture medium relative to vehicle treated cells (Fig. 7,8). Similarly, when 2AG was biosynthesized *in situ* by addition of ionomycin to LPS-primed macrophages, the levels of 2AG and PG-Gs were enhanced by CPO pretreatment of cells (Fig. 9B). However, pretreatment with PO did not yield a similar enhancement in lipid mediators (Fig. 9C), thus pointing to another hydrolase not inhibited by PO under these conditions that can also degrade these compounds. Consistent with this result, titration of monocyte lysates with high concentrations of CPO and PO revealed that CPO was a more effective inhibitor of 2AG hydrolysis activity than PO (Supplementary Fig. 3A), which is actually consistent with the data in Fig. 3 and suggestive of a role for a PO-insensitive MAGL-like enzyme. As already mentioned above, it seems unlikely that MAGL has a role because of the low amounts of this enzyme in THP1 cells. Thus, another obvious candidate is the 31-32kDa enzyme identified by activity profiling. This protein may contribute to hydrolysis of 2AG and PG-Gs generated *in situ* and may be differentially inhibited by CPO and PO in the same manner that MAGL is. However, activity profiling of the 31-32kDa enzyme in both lysates and intact cells indicates that it is not particularly sensitive to inhibition by either CPO or PO (Supplementary Fig.1). Yet there may be subtle differences in the inhibition of the 31-32kDa enzyme by oxons that cannot be discerned by activity profiling with FP-biotin. A next logical step will be to purify and identify this protein, followed by its recombinant expression to identify compounds that can inactivate its activity.

The difference observed in the PO-mediated stabilization of PG-Gs in THP1 macrophages when using exogenous 2AG or ionomycin to stimulate their production (Fig. 8 and 9C) might be caused by the larger amounts of PG-Gs likely generated from exogenous 2AG treatment as compared to the ionomycin treatment. Consequently, after addition of exogenous 2AG to the culture medium, intracellular concentrations of PG-Gs may reach levels that saturate the PO-insensitive MAGL-like enzyme resulting in their accumulation in the culture medium. By contrast, in the case of ionomycin-induced PG-G formation, the concentrations of PG-Gs available to the PO-insensitive MAGL-like enzyme are likely not saturating and PG-Gs are efficiently degraded (and thus do not accumulate in the culture medium).

The possibility that exposure of macrophages to OP insecticides can interfere with endocannabinoid production and its downstream COX-mediated metabolites suggests a novel role for these xenobiotics in vascular wall dysfunction. Consistent with this premise, Nomura et al. (47) showed that dual blockade of MAGL and FAAH by organophosphorus agents caused ten-fold elevations in mouse brain levels of both 2AG and AEA. Consequently, CB1-dependent behavioral effects were elicited. Interestingly, based on

activity-based proteomic profiling, MAGL and FAAH are much more abundant than CES in mouse brain; MAGL accounts for ~85% of the 2AG hydrolase activity in brain with the remaining 15% attributed to ABHD6 and ABHD12 (48). These data indicate that CES do not have a role in the regulation of 2AG in the central nervous system. However, we speculate that CES-regulated endocannabinoid metabolism may be an important metabolic pathway in specific cell types within peripheral tissues, such as macrophages found in vessel walls. Consistent with this premise, we also showed that cholesterol-loaded THP1 macrophages can produce significant quantities of 2AG, and that exposure to oxon metabolites resulted in concentration dependent increases in 2AG levels in the culture medium (Supplementary Fig. 7).

We hypothesize that the endocannabinoid tone of vessel wall macrophages may be significantly perturbed by chronic exposure to bioactive OP metabolites, and an activated endocannabinoid system can therefore modulate cholesterol metabolism in macrophages. In support of this idea, patients with coronary artery disease were found to have elevated levels of blood endocannabinoids and increased expression of CB1 receptors in coronary atheromas, thus an activated ECS was demonstrated in this disease state (42). Further, CB1 receptor blockade by rimonabant (a CB1 antagonist) caused anti-inflammatory effects in cultured THP1 macrophages, which might be beneficial in terms of atheroprotection (42). Conversely, activation of macrophage CB1 receptors by a selective agonist, AM-251, was shown to stimulate CD36 expression and to downregulate ABCA1 expression (43), thus enhancing a pro-atherogenic phenotype. In contrast to evidence indicating that macrophage CB1 receptor activation might prove atherogenic, activation of macrophage CB2 receptors may be anti-inflammatory and atheroprotective (49). Future studies will be required to determine if perturbed endocannabinoid homeostasis caused by chronic pesticide exposure leads to adverse outcomes, such as increased plaque formation in vessel walls. However, the results of this study demonstrate that the human THP1 macrophage cell line can metabolize 2AG and its PG-G metabolites, and that CES1 has a prominent role in their degradation. Furthermore, whether CES1 and CES2 contribute to the metabolism of 2AG in the liver and intestinal tract, respectively, should also be explored, particularly in light of the abundant expression of these isoforms in these tissues.

In conclusion, human CES1 and CES2 can hydrolyze 2AG and its COX-derived PG-G metabolites. CES1 is responsible in part for the 2AG and PG-G hydrolase activities present in THP1 monocytes/macrophages, although with regard to 2AG metabolism other hydrolase(s) also play a significant role. Studies to identify these hydrolases are currently on going. In addition, when 2AG and PG-Gs were formed *in situ* by macrophages, the amounts of these lipid mediators were significantly elevated (stabilized) by pre-treatment of cells with a non-specific hydrolase inhibitor, CPO. These findings suggest that environmental toxicants may interfere with endocannabinoid metabolic pathways in macrophages, which may have implications for disease development.

Supplementary Material

Refer to Web version on PubMed Central for supplementary material.

Acknowledgments

Research support was provided by NIH 1R15ES015348-01A1 and 3R15ES015348-01A1S1 (M.K.R.) and the American Lebanese Syrian Associated Charities (ALSAC) and St. Jude Children's Research Hospital (SJCRH) (P.M.P.). Ms. Claire Dagre and Mr. Antonio B. Ward are gratefully acknowledged for performing enzyme activity assays and serine hydrolase activity profiling experiments.

Abbreviations

AA	arachidonic acid
2AG	2-arachidonoylglycerol
CES1	carboxylesterase 1
CES2	carboxylesterase 2
CPO	chlorpyrifos oxon
CVD	cardiovascular disease
ECS	endocannabinoid system
FAAH	fatty-acid amide hydrolase
MAGL	monoacylglycerol hydrolase
PO	paraoxon
***p*NPV**	*p*-nitrophenyl valerate
PG-G	prostaglandin glyceryl esters
PGE_2-G	prostaglandin E2 glyceryl ester
$PGF_{2\alpha}$-G	prostaglandin $F_{2\alpha}$ glyceryl ester
S-3030	thieno[3,2-e][1]benzothiophene-4,5-dione

References

(1). Di Marzo V. Targeting the endocannabinoid system: to enhance or reduce? Nat. Rev. Drug Discov. 2008; 7:438–455. [PubMed: 18446159]

(2). Piomelli D. The molecular logic of endocannabinoid signalling. Nat. Rev. Neurosci. 2003; 4:873–884. [PubMed: 14595399]

(3). Pacher P, Steffens S. The emerging role of the endocannabinoid system in cardiovascular disease. Semin. Immunopathol. 2009; 31:63–77. [PubMed: 19357846]

(4). Rouzer CA, Tranguch S, Wang H, Zhang H, Dey SK, Marnett LJ. Zymosan-induced glycerylprostaglandin and prostaglandin synthesis in resident peritoneal macrophages: roles of cyclooxygenase-1 and -2. Biochem. J. 2006; 399:91–99. [PubMed: 16787386]

(5). Kozak KR, Rowlinson SW, Marnett LJ. Oxygenation of the endocannabinoid, 2-arachidonylglycerol, to glyceryl prostaglandins by cyclooxygenase-2. J. Biol. Chem. 2000; 275:33744–33749. [PubMed: 10931854]

(6). Snider NT, Walker VJ, Hollenberg PF. Oxidation of the endogenous cannabinoid arachidonoyl ethanolamide by the cytochrome P450 monooxygenases: physiological and pharmacological implications. Pharmacol. Rev. 2010; 62:136–154. [PubMed: 20133390]

(7). Rouzer CA, Marnett LJ. Glycerylprostaglandin synthesis by resident peritoneal macrophages in response to a zymosan stimulus. J. Biol. Chem. 2005; 280:26690–26700. [PubMed: 15917246]

(8). Rouzer CA, Marnett LJ. Non-redundant functions of cyclooxygenases: oxygenation of endocannabinoids. J. Biol. Chem. 2008; 283:8065–8069. [PubMed: 18250160]

(9). Nirodi CS, Crews BC, Kozak KR, Morrow JD, Marnett LJ. The glyceryl ester of prostaglandin E2 mobilizes calcium and activates signal transduction in RAW264.7 cells. Proc. Natl. Acad. Sci. U S A. 2004; 101:1840–1845. [PubMed: 14766978]

(10). Hu SS, Bradshaw HB, Chen JS, Tan B, Walker JM. Prostaglandin E2 glycerol ester, an endogenous COX-2 metabolite of 2-arachidonoylglycerol, induces hyperalgesia and modulates NFkappaB activity. Br. J. Pharmacol. 2008; 153:1538–1549. [PubMed: 18297109]

(11). Dol-Gleizes F, Paumelle R, Visentin V, Marés AM, Desitter P, Hennuyer N, Gilde A, Staels B, Schaeffer P, Bono F. Rimonabant, a selective cannabinoid CB1 receptor antagonist, inhibits atherosclerosis in LDL receptor-deficient mice. Arterioscler. Thromb. Vasc. Biol. 2009; 29:12–18. [PubMed: 18845788]

(12). Steffens S, Veillard NR, Arnaud C, Pelli G, Burger F, Staub C, Karsak M, Zimmer A, Frossard JL, Mach F. Low dose oral cannabinoid therapy reduces progression of atherosclerosis in mice. Nature. 2005; 434:782–786. [PubMed: 15815632]

(13). Ahn K, McKinney MK, Cravatt BF. Enzymatic pathways that regulate endocannabinoid signaling in the nervous system. Chem. Rev. 2008; 108:1687–1707. [PubMed: 18429637]

(14). Satoh T, Hosokawa M. The mammalian carboxylesterases: from molecules to functions. Annu. Rev. Pharmacol. Toxicol. 1998; 38:257–288. [PubMed: 9597156]

(15). Bencharit S, Morton CL, Hyatt JL, Kuhn P, Danks MK, Potter PM, Redinbo MR. Crystal structure of human carboxylesterase 1 complexed with the Alzheimer's drug tacrine. From binding promiscuity to selective inhibition. Chem. Biol. 2003; 10:341–349. [PubMed: 12725862]

(16). Bencharit S, Edwards CC, Morton CL, Howard-Williams EL, Kuhn P, Potter PM, Redinbo MR. Multisite promiscuity in the processing of endogenous substrates by human carboxylesterase 1. J. Mol. Biol. 2006; 363:201–214. [PubMed: 16962139]

(17). Sogorb MA, Vilanova E. Enzymes involved in the detoxification of organophosphorus, carbamate and pyrethroid insecticides through hydrolysis. Toxicol. Lett. 2002; 128:215–228. [PubMed: 11869832]

(18). Ross MK, Borazjani A, Edwards CC, Potter PM. Hydrolytic metabolism of pyrethroids by human and other mammalian carboxylesterases. Biochem. Pharmacol. 2006; 71:657–669. [PubMed: 16387282]

(19). Nishi K, Huang H, Kamita SG, Kim IH, Morisseau C, Hammock BD. Characterization of pyrethroid hydrolysis by the human liver carboxylesterases hCE-1 and hCE-2. Arch. Biochem. Biophys. 2006; 445:115–123. [PubMed: 16359636]

(20). Sanghani SP, Sanghani PC, Schiel MA, Bosron WF. Human carboxylesterases: an update on CES1, CES2 and CES3. Protein Pept. Lett. 2009; 16:1207–14. [PubMed: 19508181]

(21). Ross MK, Crow JA. Role of carboxylesterases in xenobiotic and endobiotic metabolism. J. Biochem. Mol. Toxicol. 2007; 21:187–196. [PubMed: 17936933]

(22). Godin SJ, Crow JA, Scollon EJ, Hughes MF, DeVito MJ, Ross MK. Identification of rat and human cytochrome P450 isoforms and a rat serum esterase that metabolize the pyrethroid insecticides deltamethrin and esfenvalerate. Drug Metab. Dispos. 2007; 35:1664–1671. [PubMed: 17576809]

(23). Schwer H, Langmann T, Daig R, Becker A, Aslanidis C, Schmitz G. Molecular cloning and characterization of a novel putative carboxylesterase, present in human intestine and liver. Biochem. Biophys. Res. Commun. 1997; 233:117–120. [PubMed: 9144407]

(24). Sun A, Jiang Y, Wang X, Liu Q, Zhong F, He Q, Guan W, Li H, Sun Y, Shi L, Yu H, Yang D, Xu Y, Song Y, Tong W, Li D, Lin C, Hao Y, Geng C, Yun D, Zhang X, Yuan X, Chen P, Zhu Y, Li Y, Liang S, Zhao X, Liu S, He F. Liverbase: a comprehensive view of human liver biology. J. Proteome Res. 2010; 9:50–8. [PubMed: 19670857]

(25). Ghosh S, Zhao B, Bie J, Song J. Macrophage cholesteryl ester mobilization and atherosclerosis. Vascul. Pharmacol. 2010; 52:1–10. [PubMed: 19878739]

(26). Center for Disease Control and Prevention. 2007. www.cdc.gov/exposurereport/pdf/thirdreport.pdf, p. 375

(27). Casida JE. Pest toxicology: the primary mechanisms of pesticide action. Chem. Res. Toxicol. 2009; 22:609–619. [PubMed: 19284791]

(28). Hyatt JL, Wadkins RM, Tsurkan L, Hicks LD, Hatfield MJ, Edwards CC, Ross CR 2nd, Cantalupo SA, Crundwell G, Danks MK, Guy RK, Potter PM. Planarity and constraint of the carbonyl groups in 1,2-diones are determinants for selective inhibition of human carboxylesterase 1. J Med. Chem. 2007; 50:5727–5734. [PubMed: 17941623]

(29). Morton CL, Potter PM. Comparison of Escherichia coli, Saccharomyces cerevisiae, Pichia pastoris, Spodoptera frugiperda, and COS7 cells for recombinant gene expression. Application to a rabbit liver carboxylesterase. Mol. Biotechnol. 2000; 16:193–202. [PubMed: 11252804]

(30). Hatfield M,J, Tsurkan L, Hyatt JL, Yu X, Edwards CC, Hicks LD, Wadkins RM, Potter PM. Biochemical and molecular analysis of carboxylesterase-mediated hydrolysis of cocaine and heroin. Br. J. Pharmacol. 2010 in press.

(31). Crow JA, Middleton BL, Borazjani A, Hatfield MJ, Potter PM, Ross MK. Inhibition of carboxylesterase 1 is associated with cholesteryl ester retention in human THP-1 monocyte/macrophages. Biochim. Biophys. Acta. (Mol. Cell Biol. Lipids). 2008; 1781:643–654.

(32). Kingsley PJ, Marnett LJ. LC-MS-MS analysis of neutral eicosanoids. Methods Enzymol. 2007; 433:91–112. [PubMed: 17954230]

(33). Vila A, Rosengarth A, Piomelli D, Cravatt B, Marnett LJ. Hydrolysis of prostaglandin glycerol esters by the endocannabinoid-hydrolyzing enzymes, monoacylglycerol lipase and fatty acid amide hydrolase. Biochemistry. 2007; 46:9578–9585. [PubMed: 17649977]

(34). Long JZ, Li W, Booker L, Burston JJ, Kinsey SG, Schlosburg JE, Pavón FJ, Serrano AM, Selley DE, Parsons LH, Lichtman AH, Cravatt BF. Selective blockade of 2-arachidonoylglycerol hydrolysis produces cannabinoid behavioral effects. Nat. Chem. Biol. 2009; 5:37–44. [PubMed: 19029917]

(35). Long JZ, Nomura DK, Cravatt BF. Characterization of monoacylglycerol lipase inhibition reveals differences in central and peripheral endocannabinoid metabolism. Chem. Biol. 2009; 16:744–753. [PubMed: 19635411]

(36). Di Marzo V, Petrosino S. Endocannabinoids and the regulation of their levels in health and disease. Curr. Opin. Lipidol. 2007; 18:129–140. [PubMed: 17353660]

(37). Kunos G, Osei-Hyiaman D, Liu J, Godlewski G, Bátkai S. Endocannabinoids and the control of energy homeostasis. J. Biol. Chem. 2008; 283:33021–33025. [PubMed: 18694938]

(38). Richie-Jannetta R, Nirodi CS, Crews BC, Woodward DF, Wang JW, Duff PT, Marnett LJ. Structural determinants for calcium mobilization by prostaglandin E2 and prostaglandin F2alpha glyceryl esters in RAW 264.7 cells and H1819 cells. Prostaglandins Other Lipid Mediat. 2010; 92:19–24. [PubMed: 20152925]

(39). Streit TM, Borazjani A, Lentz S, Wierdl M, Potter PM, Gwaltney SR, Ross MK. Evaluation of the ‘side-door’ in carboxylesterase-mediated catalysis and inhibition. Biol. Chem. 2008; 389:149–162. [PubMed: 18163883]

(40). Kozak KR, Crews BC, Ray JL, Tai HH, Morrow JD, Marnett LJ. Metabolism of prostaglandin glycerol esters and prostaglandin ethanolamides in vitro and in vivo. J. Biol. Chem. 2001; 276:36993–36998. [PubMed: 11447235]

(41). Li B, Sedlacek M, Manoharan I, Boopathy R, Duysen EG, Masson P, Lockridge O. Butyrylcholinesterase, paraoxonase, and albumin esterase, but not carboxylesterase, are present in human plasma. Biochem Pharmacol. 2005; 70:1673–1684. [PubMed: 16213467]

(42). Sugamura K, Sugiyama S, Nozaki T, Matsuzawa Y, Izumiya Y, Miyata K, Nakayama M, Kaikita K, Obata T, Takeya M, Ogawa H. Activated endocannabinoid system in coronary artery disease and antiinflammatory effects of cannabinoid 1 receptor blockade on macrophages. Circulation. 2009; 119:28–36. [PubMed: 19103987]

(43). Jiang LS, Pu J, Han ZH, Hu LH, He B. Role of activated endocannabinoid system in regulation of cellular cholesterol metabolism in macrophages. Cardiovasc. Res. 2009; 81:805–813. [PubMed: 19074161]

(44). Han KH, Lim S, Ryu J, Lee CW, Kim Y, Kang JH, Kang SS, Ahn YK, Park CS, Kim JJ. CB1 and CB2 cannabinoid receptors differentially regulate the production of reactive oxygen species by macrophages. Cardiovasc. Res. 2009; 84:378–386. [PubMed: 19596672]

(45). Mach F, Steffens S. The role of the endocannabinoid system in atherosclerosis. J. Neuroendocrinol. 2008; 20(Suppl. 1):53–57. [PubMed: 18426500]

(46). Hao MX, Jiang LS, Fang NY, Pu J, Hu LH, Shen LH, Song W, He B. The cannabinoid WIN55,212-2 protects against oxidized LDL-induced inflammatory response in murine macrophages. J. Lipid Res. 2010 Epub ahead of print.

(47). Nomura DK, Blankman JL, Simon GM, Fujioka K, Issa RS, Ward AM, Cravatt BF, Casida JE. Activation of the endocannabinoid system by organophosphorus nerve agents. Nature Chem. Biol. 2008; 4:373–378. [PubMed: 18438404]

(48). Blankman JL, Simon GM, Cravatt BF. A comprehensive profile of brain enzymes that hydrolyze the endocannabinoid 2-arachidonoylglycerol. Chem. Biol. 2007; 14:1347–1156. [PubMed: 18096503]

(49). Immenschuh S. Endocannabinoid signalling as an anti-inflammatory therapeutic target in atherosclerosis: does it work? Cardiovasc. Res. 2009; 84:341–342. [PubMed: 19819883]

(50). Rouzer CA, Ghebreselasie K, Marnett LJ. Chemical stability of 2-arachidonoylglycerol under biological conditions. Chem. Phys. Lipids. 2002; 119:69–82. [PubMed: 12270674]

(51). Kidd D, Liu Y, Cravatt BF. Profiling serine hydrolase activities in complex proteomes. Biochemistry. 2001; 40:4005–4015. [PubMed: 11300781]

(52). Li W, Blankman JL, Cravatt BF. A functional proteomic strategy to discover inhibitors for uncharacterized hydrolases. J. Am. Chem. Soc. 2007; 129:9594–9595. [PubMed: 17629278]

(53). Di Marzo V, Bisogno T, De Petrocellis L, Melck D, Orlando P, Wagner JA, Kunos G. Biosynthesis and inactivation of the endocannabinoid 2-arachidonoylglycerol in circulating and tumoral macrophages. Eur. J. Biochem. 1999; 264:258–267. [PubMed: 10447696]

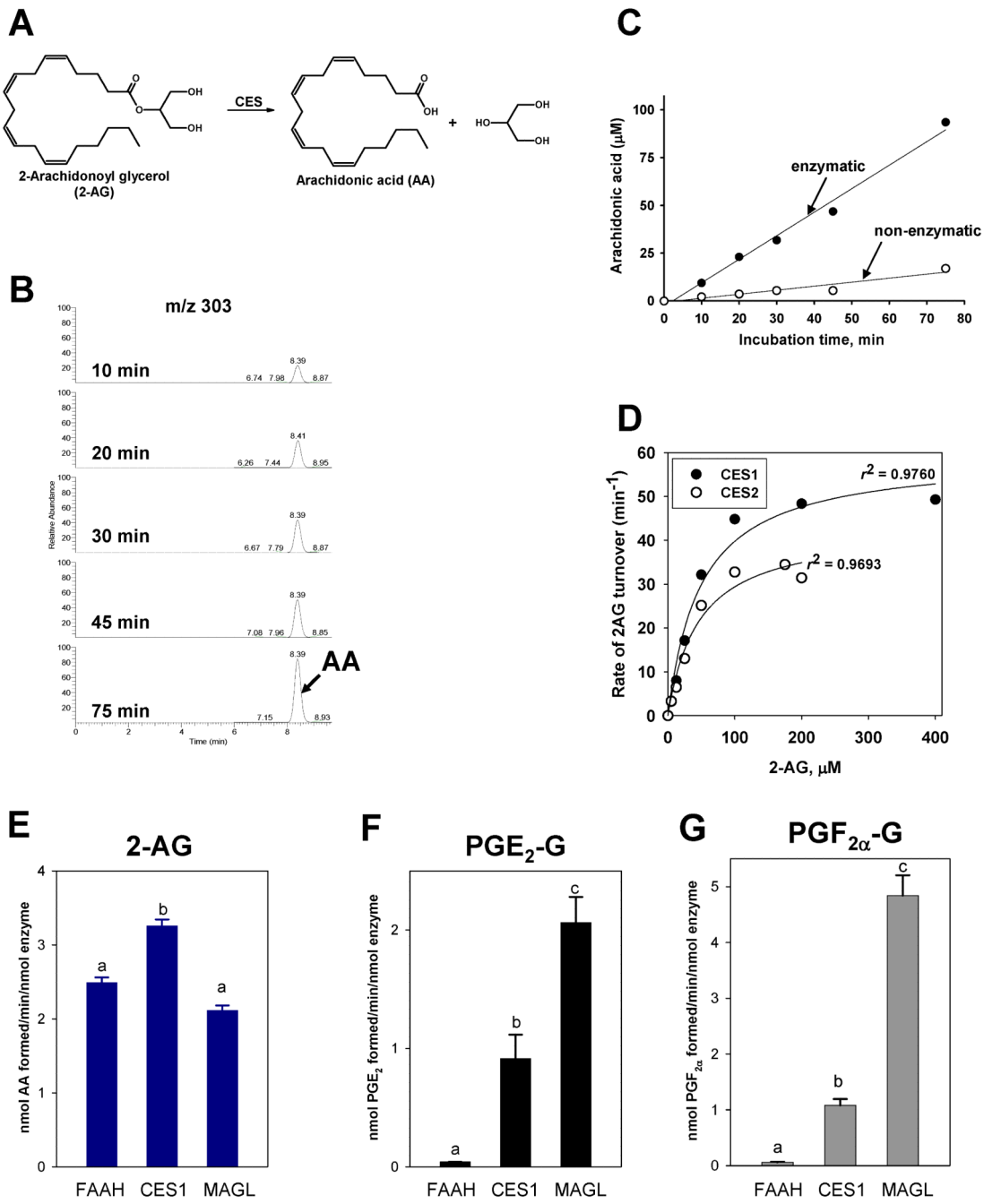

Figure 1.

Hydrolysis of 2AG and PG-Gs by recombinant human CES 1 and 2. (**A**) Chemical scheme of 2AG hydrolysis. (**B**) LC-MS chromatograms of arachidonic acid (AA, m/z 303) obtained when 2AG was incubated with CES1 for 10-75 min. (**C**) Time course of AA formation when 2AG (250μM) was incubated in the presence (enzymatic) or absence (non-enzymatic) of CES1. (**D**) Substrate concentration vs. velocity (rate of 2AG turnover) curves for human recombinant CES1 and CES2. Curves are representative of at least 3 independent experiments. (**E-G**) Comparison of the hydrolytic activities of FAAH, CES1, and MAGL

toward 2AG (10 μM), PGE_2-G (25 μM) or $PGF_{2\alpha}$-G (25 μM). Recombinant human enzymes were incubated with (**E**) 2AG (10μM), (**F**) PGE_2-G (25μM), or (**G**) $PGF_{2\alpha}$-G (25μM) for 15 min. Products were analyzed by LC-MS and quantified using internal standard (8-*iso*-$PGF_{2\alpha}$-d_4 or AA-d_8). Data represent the mean ± SD of triplicate reactions. Different lower case letters indicate statistical differences between groups ($p<0.05$, one-way ANOVA and Tukey test).

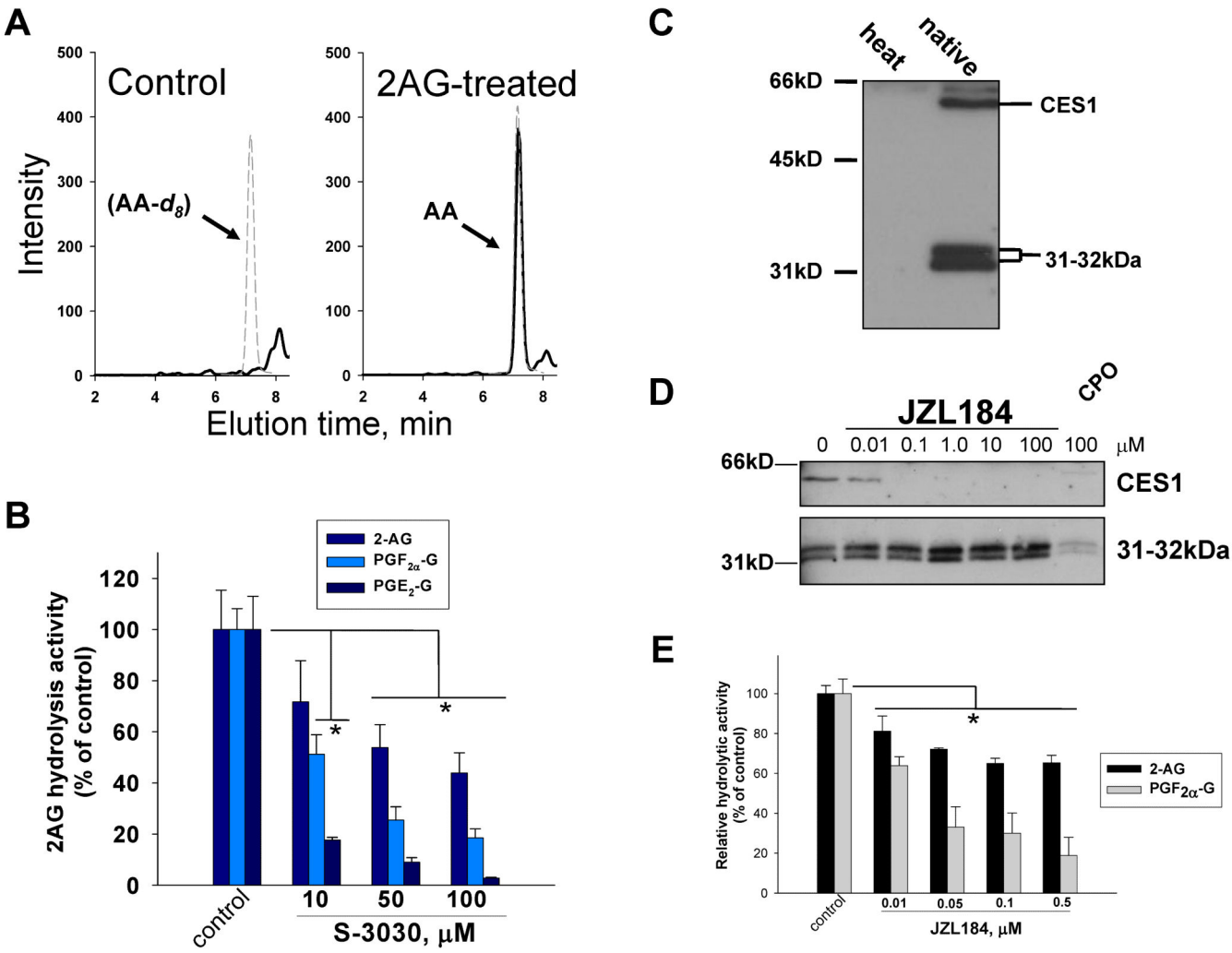

Figure 2.

THP1 monocytes hydrolyze the lipid mediators 2AG, PGE_2-G, or $PGF_{2\alpha}$-G. (**A**) Intact THP1 cells were incubated in serum-free medium in the absence (control) and presence of exogenous 2AG (10μM) for 1 h. LC-MS chromatograms are shown. Solid black line (AA, m/z 303); dashed grey line (AA-d_8, m/z 310). (**B**) Inhibition of lipid glyceryl ester metabolism in THP1 monocyte lysates by S-3030. Control THP1 lysate hydrolysis activities for 2AG, $PGF_{2\alpha}$-G, and PGE_2-G represent 2.5, 0.6, and 0.8 nmol product/min/mg protein, respectively, when using 25 μM substrate. (**C**) Serine hydrolase activity profile of THP1 monocyte lysate determined with FP-biotin (2μM, 1h, room temp). *heat* indicates lysates were boiled prior to addition of FP-biotin, *native* indicates lysates were not boiled. An endogenous biotin-containing protein is detected ~75kDa in both *heat* and *native* samples (band not shown) and is not dependent on FP-biotin treatment. (**D**) Activity profile of CES1 and 31-32kDa enzyme following incubation of THP1 lysate with JZL184 or 100μM CPO (positive control) for 30 min (37°C), followed by FP-biotin (2μM, 1h, room temp). (**E**) Inhibition of lipid glyceryl ester metabolism in THP1 monocyte lysates by JZL184. Bar graphs represent the mean ± SD of triplicate reactions. * $p<0.05$ for inhibitor-treated lysate versus vehicle-treated lysate, one-way ANOVA and Dunnett's test.

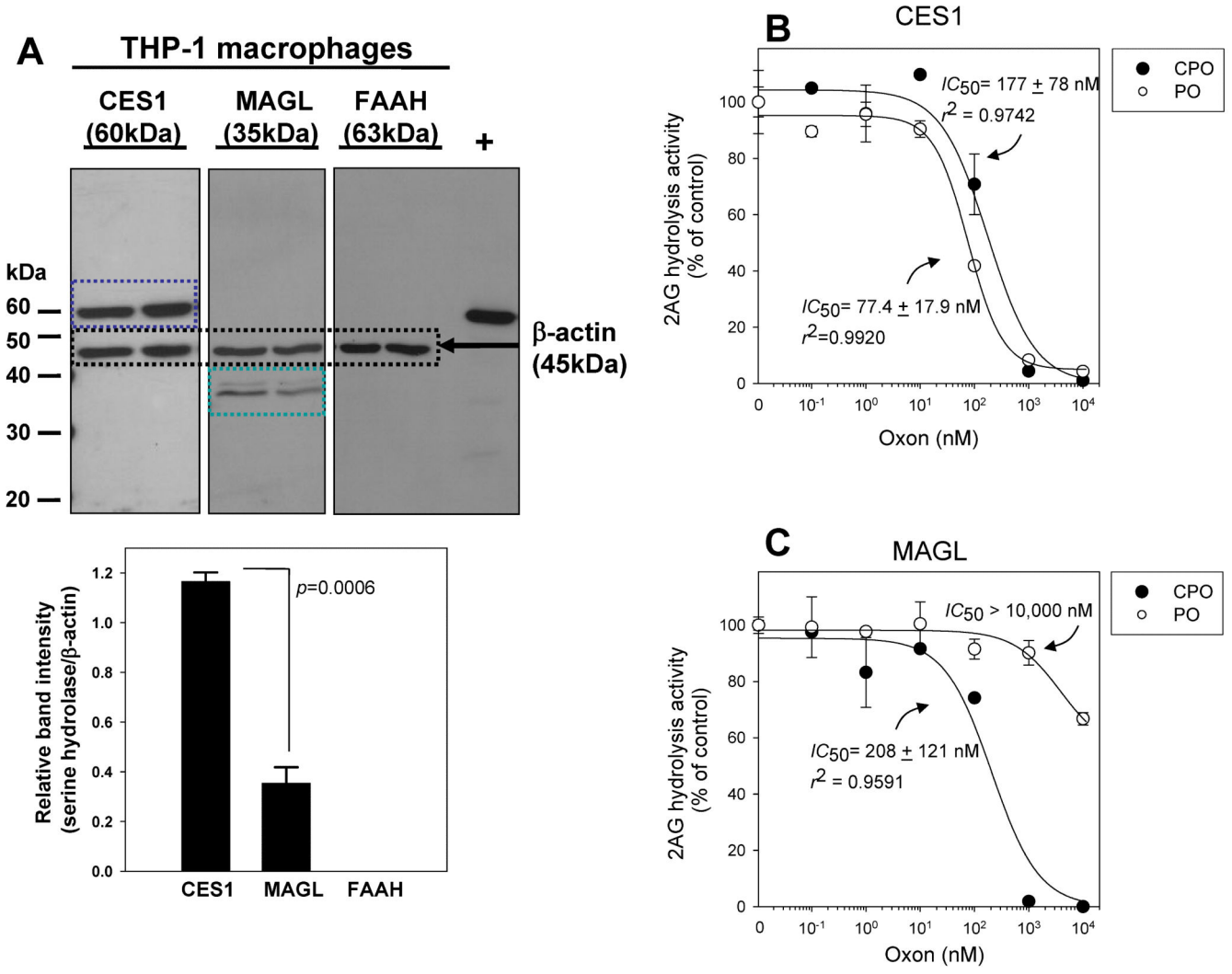

Figure 3.

Expression of 2AG hydrolytic enzymes in THP1 cells and sensitivity of CES1 and MAGL toward oxons. (**A**) THP1 macrophages express CES1 and MAGL, but do not express FAAH. PVDF membranes were probed using rabbit anti-CES1, rabbit anti-MAGL, or rabbit anti-FAAH antibodies. Antigen-antibody complexes were detected using goat anti-rabbit secondary antibody conjugated to HRP. Rabbit anti-βactin was used to verify equal protein loading (25μg per lane). +, rat liver microsomal protein used as a positive control for FAAH antibody. Normalized band intensities are shown below western blot. (**B,C**) Inhibition curves for CES1- and MAGL-mediated hydrolysis of 2AG by PO (open symbol) and CPO (closed symbol). Data represent the mean ± SD of triplicate reactions.

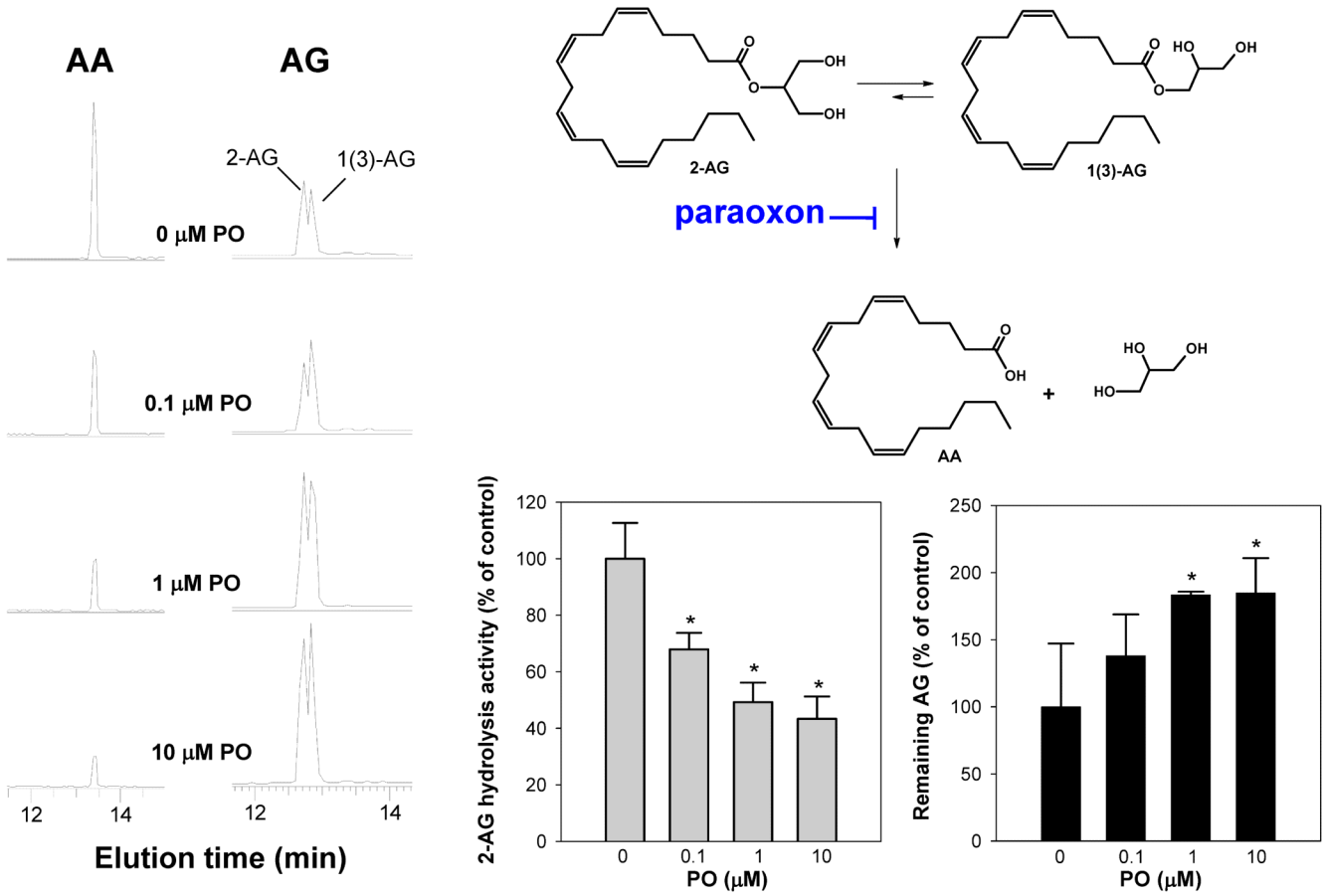

Figure 4.

Treatment of intact THP1 macrophages with paraoxon inhibits the hydrolytic metabolism of 2AG. THP1 macrophages were pretreated with increasing amounts of PO (0.1-10 μM, 30 min), followed by addition of 2AG (10 μM, 60 min). Cells and culture medium were combined, spiked with internal standard (AA-d_8), and extracted with ethyl acetate (0.1% acetic acid) for LC-MS assay. Data represent the mean ± SD of triplicate plates. * p<0.05 for inhibitor-treated cells versus vehicle-treated cells, one-way ANOVA and Dunnett's test. 2AG exists in aqueous solution as a mixture of two isomers, 2AG and 1(3)-AG (50).

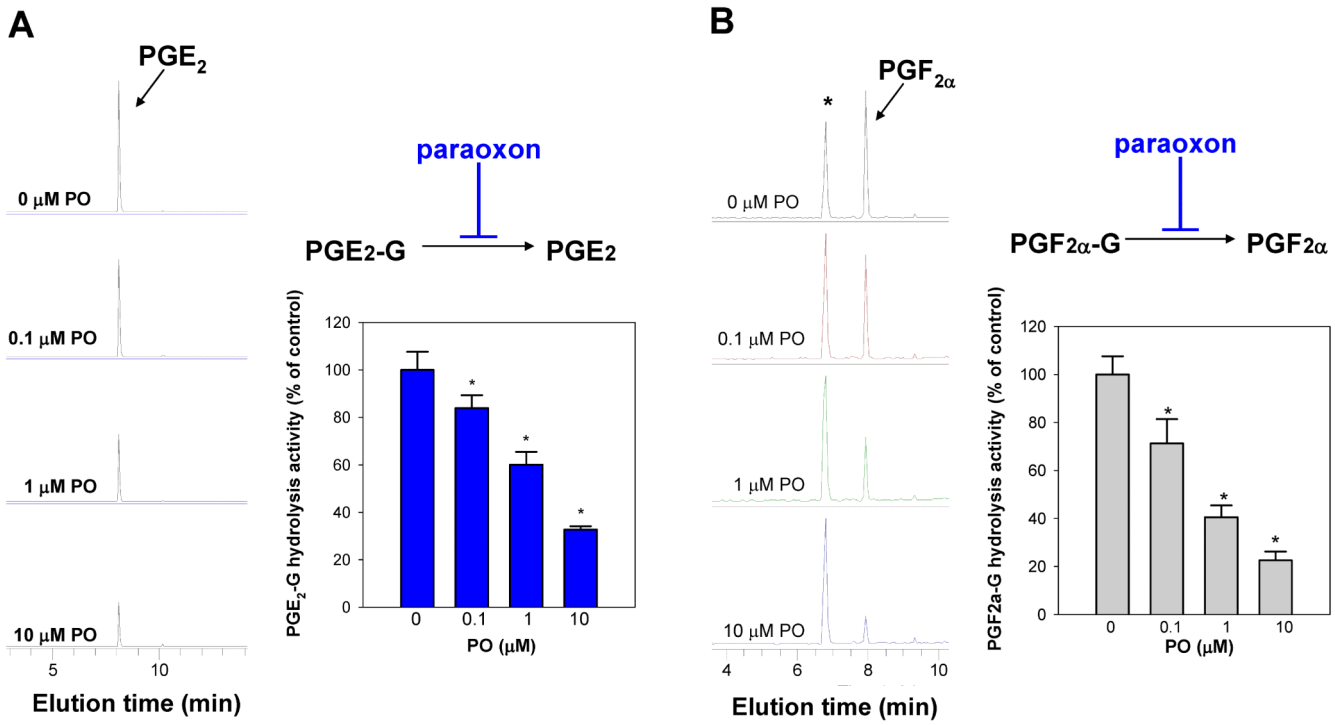

Figure 5.

Treatment of intact THP1 macrophages with paraoxon inhibits the hydrolytic metabolism of PGE_2-G and $PGF_{2\alpha}$-G. THP1 macrophages were pretreated with increasing amounts of PO (0.1-10 μM, 30 min), followed by addition of PGE_2-G (10 μM, 60 min) (**A**) or $PGF_{2\alpha}$-G (10 μM, 60 min) (**B**). Cells and culture medium were combined, spiked with internal standard (8-*iso*-$PGF_{2\alpha}$-d_4), and extracted with ethyl acetate (0.1% acetic acid) for LC-MS assay. Data represent the mean ± SD of triplicate plates. * $p<0.05$ for inhibitor-treated cells versus vehicle-treated cells, one-way ANOVA and Dunnett's test.

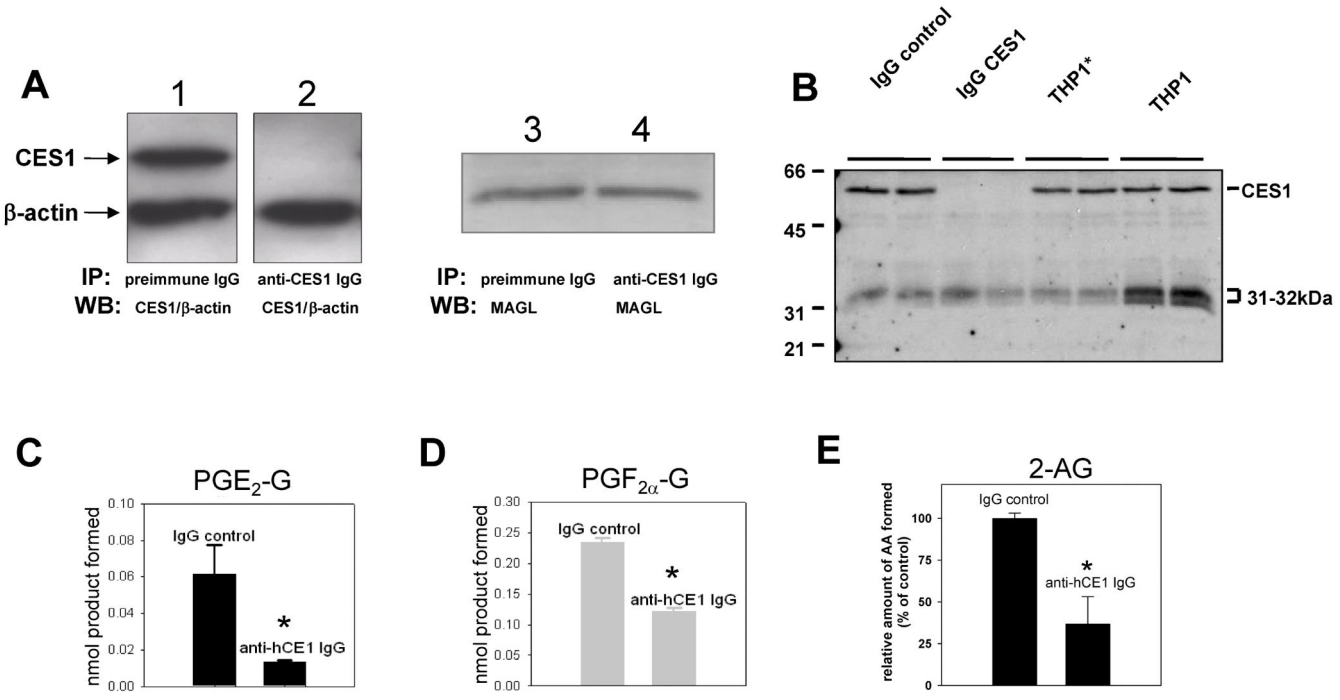

Figure 6.

Immunoprecipitation of CES1 from THP1 monocyte lysates significantly reduces the hydrolysis of lipid glyceryl esters. CES1 was immunoprecipitated from cell lysates using rabbit anti-CES1 IgG antibodies. As a negative control, lysates were incubated with preimmune IgG antibodies. (**A**) Following centrifugation of antibody-lysate incubates, aliquots of the supernatants were run on SDS-PAGE to detect CES1 and β-actin by western blot (lanes 1 and 2) or MAGL (lanes 3 and 4). β-Actin was probed to verify equal gel loading of lysate proteins. (**B**) Supernatants were also treated with FP-biotin to examine the serine hydrolase activity profile. *THP1* indicates lysates prepared in 50 mM Tris-HCl (pH 7.4) buffer, *THP1** indicates lysates were solubilized in Tris-HCl (pH 7.4) buffer containing 0.5% Brij. (**C,D**) Supernatants were incubated with fixed amounts of PG-G (25 μM) for 30 min and ethyl acetate extracts analyzed by LC-MS to determine the amounts of hydrolysis product formed (PGE_2 and $PGF_{2\alpha}$). (**E**) Alternatively, supernatants were incubated with 2AG (10 μM) for 30 min. Data are from at least two independent IP experiments, each reaction with substrate was performed in duplicate or triplicate. * $p<0.05$ for CES1-depleted lysate versus control lysate, Student's *t*-test.

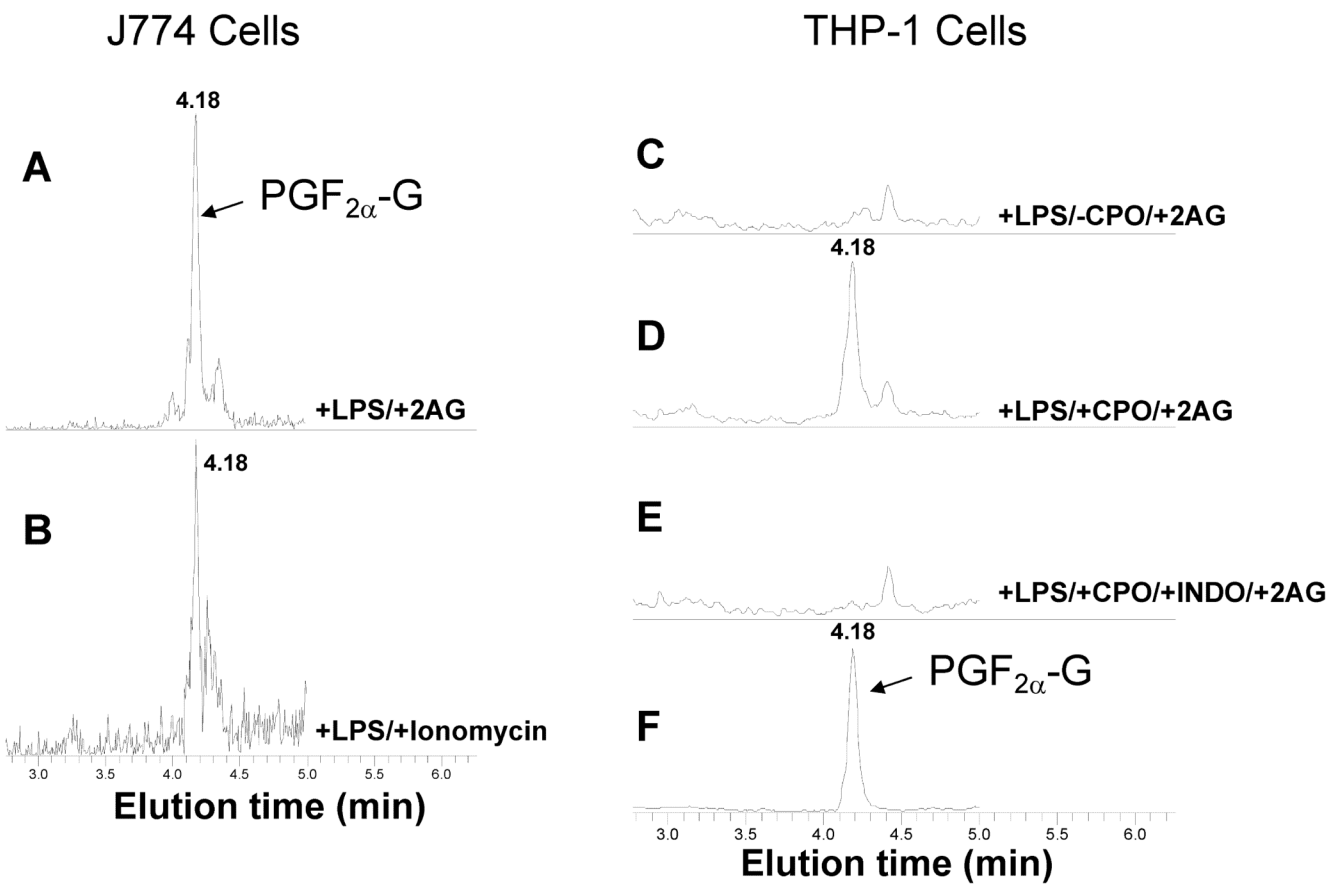

Figure 7.

Murine and human macrophage cell lines produce PG-Gs. (**A,B**) Murine J774 macrophages were primed with LPS (1 μg/ml) for 5 h, followed by addition of 2AG (10 μM) (**A**) or ionomycin (5 μM) (**B**). After 30 min, the culture medium was removed and extracted for LC-MS/MS analysis (chromatograms for $PGF_{2\alpha}$-G are shown). (**C**) Human THP1 macrophages were primed with LPS (1 μg/ml) for 5 h, followed by addition of 2AG. No PG-Gs were detected. (**D**) If macrophages were pretreated with CPO (1 μM) prior to adding 2AG, then PG-Gs were detected. (**E**) If the non-specific COX inhibitor indomethacin (3 μM) was added along with CPO prior to 2AG addition, then no PG-Gs were produced. (**F**) A chromatogram of the authentic standard of $PGF_{2\alpha}$-G is shown. Chromatograms shown are representative of three independent experiments. As seen with 2AG, PG-Gs exist in aqueous solution as a mixture of two isomers, 2-PG-G and 1(3)-PG-G (see Figure 10).

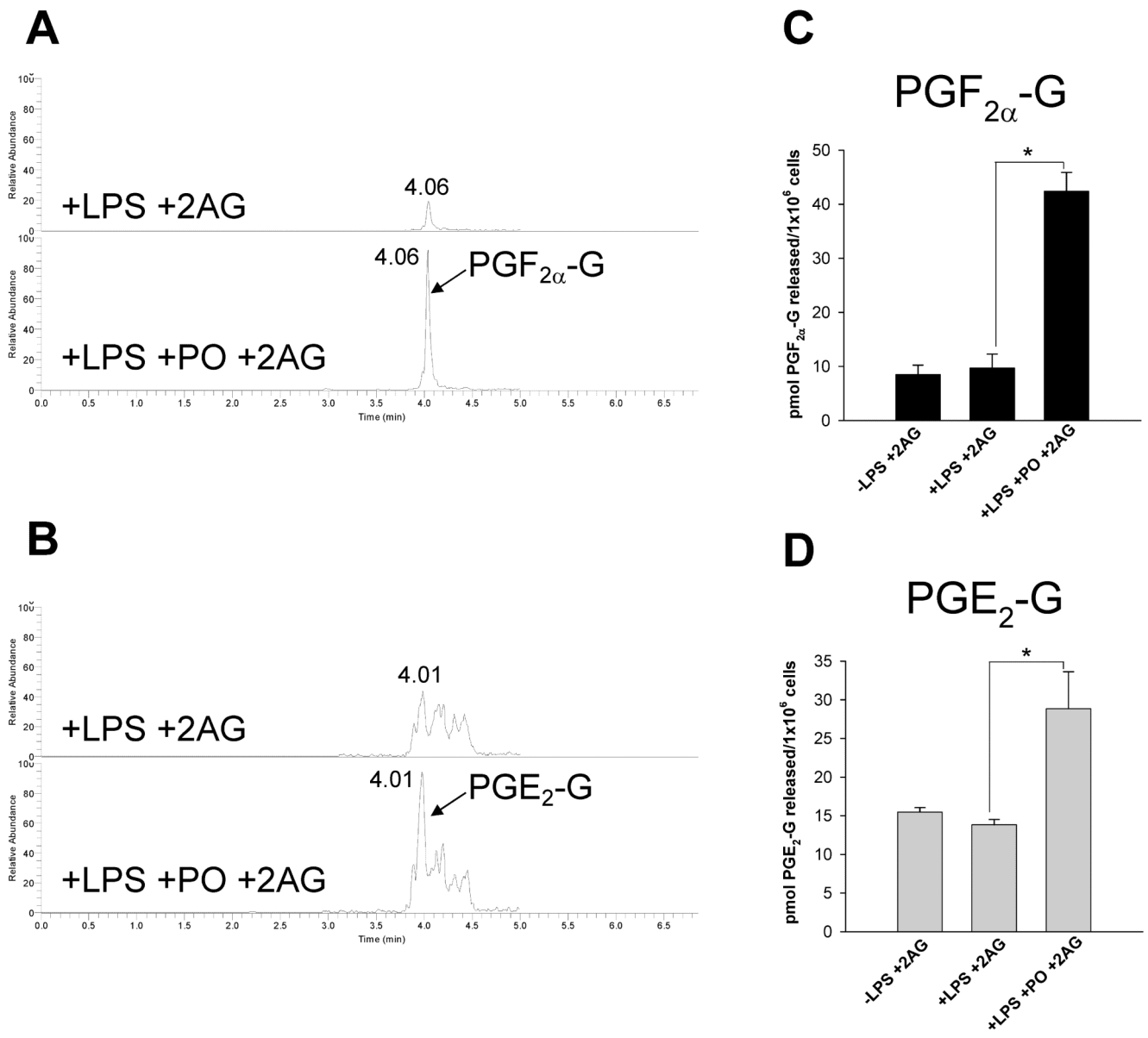

Figure 8.

PO significantly elevates the amounts of PG-Gs formed *in situ* by THP1 macrophages subsequently exposed to 2AG. THP1 macrophages were treated with lipopolysaccharide (LPS, 1 μg/ml) for 5 h. Culture medium was removed and cells pre-treated with paraoxon (PO, 1 μM) or vehicle (ethanol) in serum-free medium for 30 min. After 30 min, 2AG (10 μM) was directly added to culture medium and cells incubated for an additional 30 min. Culture medium was re-moved and extracted for LC-MS/MS analysis of $PGF_{2\alpha}$-G (**A,C**) and PGE_2-G (**B,D**). Data represent the mean ± SD of triplicate plates in a single experiment, and are representative of three independent experiments. * $p<0.05$ for PO-treated cells versus vehicle-treated cells, Student's *t*-test.

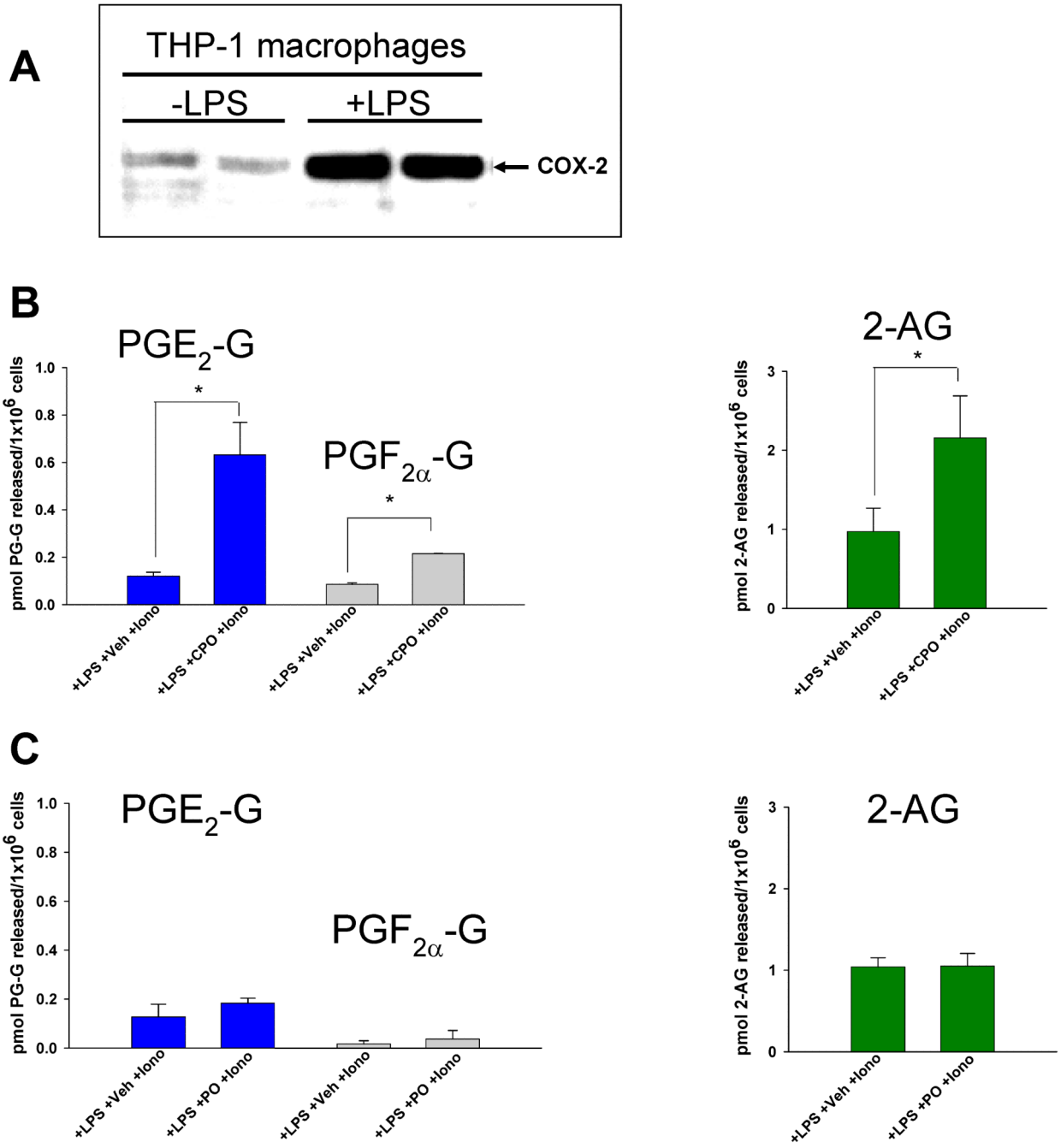

Figure 9.

CPO-pretreated THP1 macrophages have elevated ionomycin-stimulated PG-G levels. (**A**) LPS priming (1 μg/ml, 5 h) of THP1 macrophages induced COX-2, as determined by western blot. (**B**) Prereatment of macrophages with 1 μM CPO followed by ionomycin stimulation caused PG-Gs and 2AG levels to be elevated. (**C**) Prereatment of macrophages with 1 μM PO followed by ionomycin stimulation did not elevate PG-G and 2AG levels. Data represent the mean ± SD of triplicate plates in a single experiment, and are

representative of three independent experiments. * $p<0.05$ for CPO-treated cells versus vehicle-treated cells, Student's *t*-test.

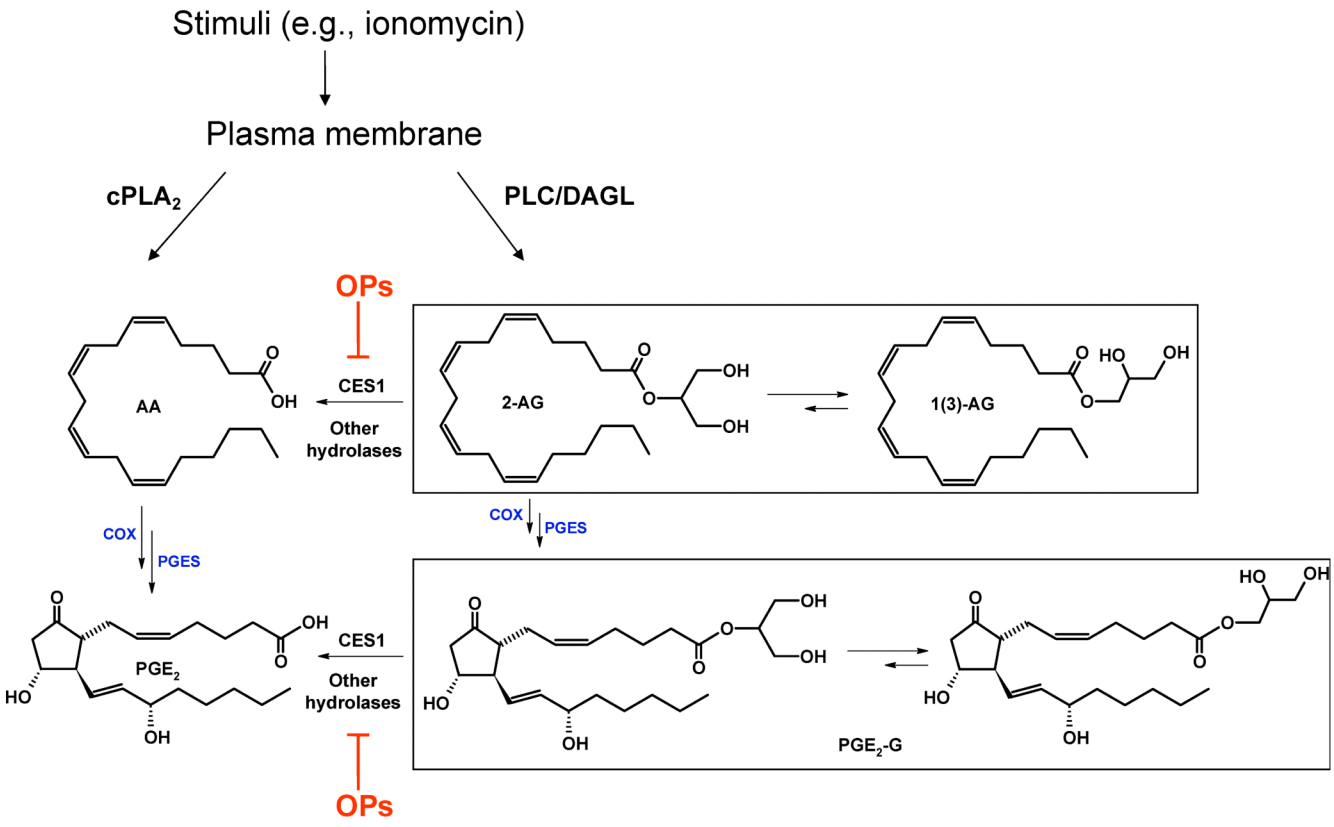

Figure 10.

Cross talk between endocannabinoids and PG-Gs in THP1 macrophages. Abbreviations: $cPLA_2$, cytosolic phospholipase A_2; PLC, phospholipase C; PLD, phospholipase D; DAGL, diacylglycerol lipase; COX, cyclooxygenase; PGES, prostaglandin E_2 synthase.

Table 1

Steady-state kinetic parameters for hydrolysis of 2AG and PG-Gs by recombinant human CES1 and CES2

	Human CES1		
Substrate	**k_{cat} (min^{-1})**	**K_m (μM)**	**k_{cat}/K_m (min^{-1} $μM^{-1}$)**
2AG	59 ± 4[a]	49 ± 11	(1.2)
$PGF_{2α}$-G	29 ± 3.5[a,b]	93 ± 43	0.49 ± 0.18[a] (0.31)
PGE_2-G	90 ± 16[b]	250 ± 60	0.37 ± 0.05 (0.36)

	Human CES2		
Substrate	**k_{cat} (min^{-1})**	**K_m (μM)**	**k_{cat}/K_m (min^{-1} $μM^{-1}$)**
2AG	43 ± 4[a]	46 ± 13	(0.93)
$PGF_{2α}$-G	49 ± 5.4[a]	35 ± 4.1	1.5 ± 0.30[a,b] (1.4)
PGE_2-G	150 ± 81	705 ± 380	0.23 ± 0.03[b] (0.21)

Values are the average ± SE of 2-4 independent experiments. k_{cat}/K_m values in parentheses are obtained using the mean values for each kinetic parameter.

[a] $p<0.05$ for CES1 versus CES2 when using the same substrate, Student's *t*-test

[b] $p<0.05$ for PGF2-G versus PGE2-G when using the same enzyme, Student's *t*-test